genes

MDPI

Review

Schizosaccharomyces pombe Assays to Study Mitotic Recombination Outcomes

Hannah M. Hylton [1,†], Bailey E. Lucas [2,†] and Ruben C. Petreaca [3,*]

1 Biology Program, The Ohio State University, Marion, OH 43302, USA; hylton.167@buckeyemail.osu.edu
2 The Ohio State University Comprehensive Cancer Center, Columbus, OH 43210, USA; lucas.637@osu.edu
3 Department of Molecular Genetics, The Ohio State University, Marion, OH 43302, USA
* Correspondence: petreaca.1@osu.edu
† Denotes equal contribution.

Received: 20 December 2019; Accepted: 7 January 2020; Published: 10 January 2020

Abstract: The fission yeast—*Schizosaccharomyces pombe*—has emerged as a powerful tractable system for studying DNA damage repair. Over the last few decades, several powerful in vivo genetic assays have been developed to study outcomes of mitotic recombination, the major repair mechanism of DNA double strand breaks and stalled or collapsed DNA replication forks. These assays have significantly increased our understanding of the molecular mechanisms underlying the DNA damage response pathways. Here, we review the assays that have been developed in fission yeast to study mitotic recombination.

Keywords: mitotic recombination; DNA replication; double strand break (DSB); chromosomal rearrangements

1. Introduction

An accurate DNA damage response (DDR) is fundamentally important for cellular homeostasis. The DDR involves first detection of the damage and activation of the DNA damage checkpoints, then recruitment of the repair machinery and repair of the damage. In humans, defects in DDR can lead to a variety of syndromes and diseases [1].

The DNA double strand break (DSB) constitutes severing of the chromosome into two parts. Threatening the viability of a cell, DSBs can lead to loss of essential chromosomal regions. In multicellular organisms, unrepaired breaks may cause cells to undergo apoptosis and new cells can be regenerated [2,3]. However, inappropriate repair of breaks may give rise to translocations, deletions, duplications and inversions [4,5] which have been identified in cancer cells [6].

DSBs may be produced by endogenous or exogeneous sources but are generally repaired by the same mechanisms [7]. Most endogenous breaks occur as a consequence of replication stress. DNA replication forks can stall or collapse as they pass through heterochromatin regions [8,9], collide with RNA polymerases [10] or pass through other fragile sites characterized by repetitive elements or euchromatin to chromatin boundaries [11,12]. The recombination machinery evolved to rescue stalled or collapsed replication forks [13].

The multitude of repair mechanisms that eukaryotic cells evolved to deal with these breaks have been previously extensively reviewed [7,10,14–19] and can be generally broken into two major pathways, non-homologous end joining (NHEJ) and homologous recombination (HR). NHEJ involves localized repair of breaks with no major sequence rearrangements. Repair can result in small deletions or alterations of the sequences neighboring the break so NHEJ is considered an error-prone form of repair [20]. HR can be subdivided into several mechanisms that are both genetically and biochemically related such as single strand annealing (SSA), break induced replication (BIR) and the two closely

related gene conversion (GC) mechanisms: synthesis dependent strand annealing (SDSA) and double Holliday junction (dHJ) (Figure 1) [7]. HR has been traditionally considered error proof because it uses an intact template sequence to copy the missing or broken region although some pathways of HR can be quite mutagenic [21].

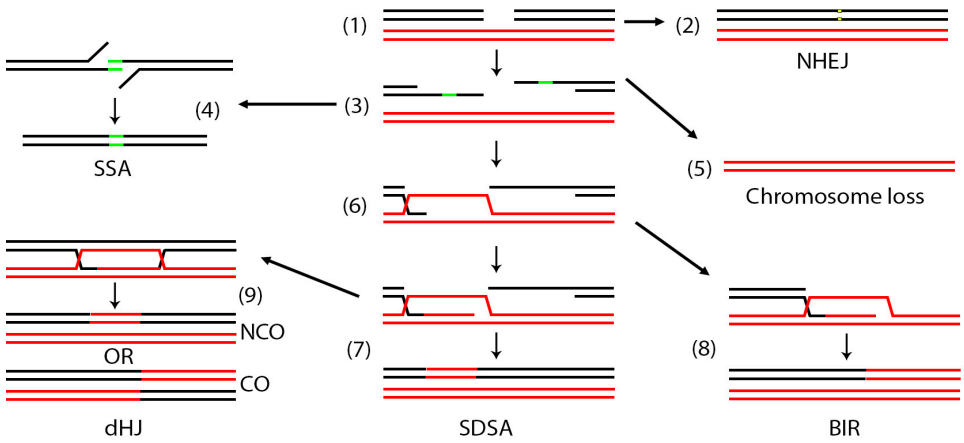

Figure 1. Cellular pathways of mitotic DNA double strand break repair. In a diploid cell, a DSB may occur in one of the two homologous chromosomes (1). The DSB may be repaired by non-homologous end joining (NHEJ) (2). When repair occurs by homologous recombination (HR), the DSB is first resected (3) to expose areas of single stranded DNA. If direct repeats (green areas) exist on the same chromosome, the break may be repaired by single strand annealing (SSA) (4). If homology is not found, the chromosome may be entirely lost (5). When homology is found elsewhere, the broken ends may invade this region (6). In synthesis dependent strand annealing (SDSA) (7) the invading strand may copy a small region then release and re-anneal. In break induced replication (BIR) (8) the invading strand may copy to the end of the red chromosome. In this case the right part of the broken black chromosome is lost. Occasionally, a more complex double Holiday junction (dHJ) may be established (9), the resolution of which can result in crossovers (CO) or non-crossovers (NCO).

Schizosaccharomyces pombe (fission yeast) diverged from *Saccharomyces cerevisiae* (budding yeast) approximately a billion years ago [22,23]. Many genes have been identified in *S. pombe* that show similarity to genes involved in human disease [24]. This is comparable to the level of conservation between *S. cerevisiae* and humans [25]. However, *S. pombe* appears to show higher conservations in chromosome structure and function genes [26] making *S. pombe* a great model system for studying chromosomal dynamics.

Specific to the study of chromosomal double strand break repair, fission yeast is great for several reasons. First, DDR genes are highly conserved from yeast to humans [27,28]. Second, in fission yeast, repetitive DNA elements, which are often a reason for endogenous breaks in human cells [29], are found only at centromeres and telomeres [30]. The overall structure of centromeres is conserved between yeast and humans. We and others have previously shown that replication trough the centromere does lead to chromosome breakage [31–35]. The presence of these repeats in only a few well characterized regions allows the better monitoring of the events that govern DSB repair. Third, haploid fission yeast has only three chromosomes [36] making it easier to track translocations and other aberrations resulting from inappropriate break repair. Fourth, fission yeast is as well suited for genetic screens as baker's yeast [37]. Finally, working with fission yeast is inexpensive and easy to learn.

A plethora of assays have been developed to study DNA damage in various systems and some are described in several recent elegant reviews [38–41]. Here, we focus on *S. pombe* and review primarily the in vivo assays that have been developed in this system to study mitotic recombination. We briefly summarize these assays and direct the reader to the original publications for more details.

2. Mini-Chromosome Assays

Mini-chromosome assays have been instrumental in elucidating many recombination pathways. Chromosome III (Ch.III), the smallest *S. pombe* chromosome, houses rDNA repeats at both ends next to the telomeres and has the longest centromere [36] (Figure 2A). Using γ irradiation, Niwa et al. [42,43] isolated a truncated Ch.III (termed Ch^{16}) in haploid yeast (Figure 2B). Unlike *S. cerevisiae* which has point centromeres [44], *S. pombe* centromeres are characterized by repetitive elements resembling higher metazoans [30]. Since both the centromere and the rDNA repeats fluctuate in number between strains, the size of Ch.III cannot be determined precisely making it approximately 3.5 Mb. Initial genetic maps estimated the centromere to be 100 Kb [45–47] but latter structural analysis identified a 110 Kb centromere [48]. The fission yeast genome sequence [24] set the centromere size at 68 Kb with the caveat that seven 6760 bp repeats were missing. The addition of these repeats to the 68 Kb region brings the size of CEN III to 110 Kb which is what PomBase (the scientific database for fission yeast) reports [49,50]. The centromere spans between the $meu27^+$ and $ppc1^+$ loci (Figure 2A).

The truncated mini-chromosome Ch^{16} should retain an intact Ch.III centromere but not have rDNA repeats. Pulse field gel electrophoresis shows that this mini-chromosome is about 530 Kb [42,43,51]. The chromosome can be maintained in haploid yeast by intra-allelic complementation between *ade6-M210* (Ch.III) and *ade6-M216* (Ch^{16}) (Figure 2A,B). Genetic mapping by Niwa et al. [42] showed that the left arm does not include the $ade10^+$ locus but the $yps1^+$ locus is present [51]. There are approximately 30 Kb between $yps1^+$ and $ade10^+$ and 84 Kb between $yps1^+$ and $meu27^+$, so it appears that the left arm is about 110 Kb. On the right arm, $ade6^+$ is 172 Kb from $ppc1^+$. Genetic mapping shows the presence of the $ags1^+$ locus (formerly $tps16^+$ [52]) 58 Kb telomere proximal from $ade6^+$ but not $tps14^+$ which is approximately 200 Kb from $ags1^+$ [42]. $cid2^+$ is within 5 Kb of $ags1^+$. Southern blotting has shown the presence of the SPCC61.05 locus 75 Kb from $ags1^+$ [53]. Thus, the right arm is about 305 Kb.

Niwa et al. determined that Ch^{16} is stable in mitotically dividing haploid cells at one copy per cell but unstable at two copies [42]. Remarkably, cells were able to simultaneously stably propagate both Ch^{16} and a 100 Kb shorter derivative (Ch^{16D1}) suggesting that yeast cells may be able to determine ploidy by the size of the chromosome. Ch^{16} loss monitored by appearance of adenine auxotrophs occurred at a frequency of 1 in 10^4 cells.

The Humphrey lab has produced several derivatives of Ch^{16} to study recombination outcomes in vivo. They initially placed the *S. cerevisiae* homothallic endonuclease (*HO*) restriction site (*MATa*) marked with the kanamycin antibiotic resistance gene (*KAN*) at the $rad21^+$ locus 27 Kb telomere distal of *ade6-M216* producing Ch^{16}-MG (Figure 2C) [54]. *KAN* confers resistance to G418 (Geneticin). Upon induction of a single DSB, gene conversion of the *KAN* locus can be monitored by screening for adenine prototrophic and G418 sensitive (ade+$G418^S$) colonies while chromosome loss will lose both markers. Long track gene conversion produces the same phenotype as chromosome loss, so it was necessary to distinguish between the two by pulse field gel electrophoresis (PFGE). Similarly, because an ade^+G418^R phenotype could result from repair by NHEJ or failure of *HO* cutting, it was necessary to sequence across the DSB site.

Ch^{16}-MG was improved by adding the $his3^+$ marker at the $cid2^+$ locus approximately 25 Kb from the *MATa* site creating Ch^{16}-MGH (Figure 2D) [53]. The advantage of this is that BIR can be investigated by monitoring the loss of both *KAN* and his^+ markers but retention of the adenine prototrophy (ade+$G418^S$his-). In BIR, the break is repaired by copying the missing information from Ch.III which is $his3^-$. PFGE followed by southern blotting showed both a larger mini-chromosome termed Ch^x and the presence of the $ade5^+$ marker, which could have only been transferred onto the Ch^{16} from Ch.III by BIR. A mini-chromosome with *MATa-HPH* marker (Ch^{16}-MHH) was also constructed which behaved identically to Ch^{16}-MGH. HPH confers resistance to hygromycin abbreviated as HYG in this paper. Bioneer has generated a deletion mutant library marked with *KanMX* [55] and this Ch^{16}-MHH chromosome is a powerful tool in screening genes that affect repair.

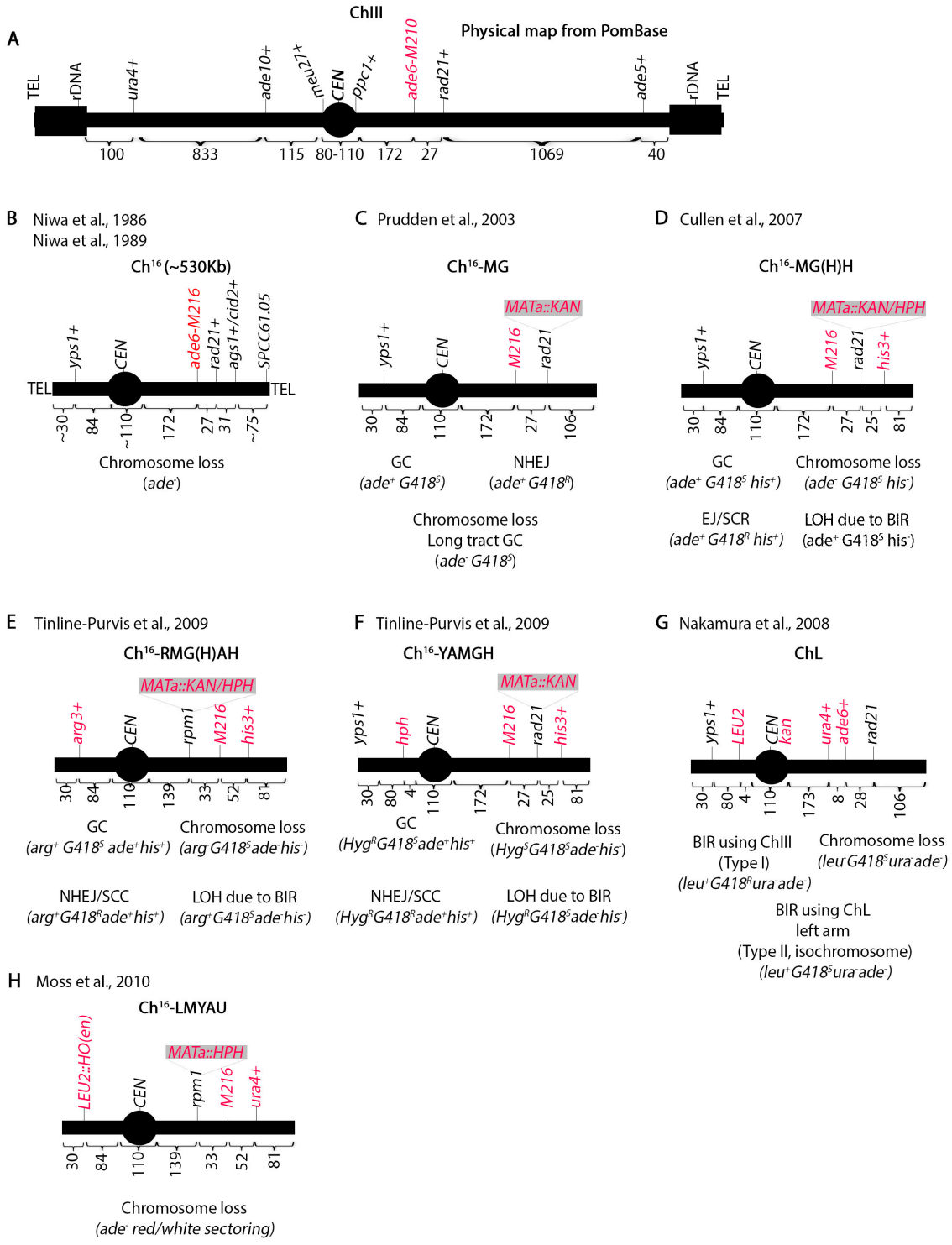

Figure 2. *S. pombe* mini-chromosome derivatives of Ch.III to study recombination. (**A**) Diagram of Chromosome III indicating the physical position of some genes. The numbers indicate kilobases. *ade6-M210* provides intra-allelic complementation with *ade6-M216*. Ch.III is approximately 3.5 Mb. (**B**) The Ch^{16} mini-chromosome isolated by Niwa et al. Ch^{16} is 0.5 Mb and lacks rDNA repeats. Chromosome loss can be monitored by appearance of adenine auxotrophs. (**C**) Ch^{16}-MG designed by Prudden et al. with the HO endonuclease restriction site at the *rad21* locus. This chromosome can monitor, gene conversion, NHEJ and chromosome loss. (**D**) Modified Ch^{16}-MG to include the *his3*$^{+}$ marker close to the right telomere which can monitor LOH due to BIR. (**E**) The *arg3+* marker was placed

on the left arm of Ch^{16}-MGH to produce Ch^{16}-RMGAH. The *arg3+* marker allows monitoring of extensive BIR that leads to loss of all markers on the right arm but retention of the left arm. (**F**) This mini-chromosome was generated to show that the outcomes of the assay in **E** were not dependent on break position. (**G**) A mini-chromosome designed to investigate recombination at centromeric repeats. (**H**) A mini-chromosome to investigate chromosome loss by red/white sectoring. The HO endonuclease is integrated in the left arm of the chromosome and marked with *LEU2*.

A third marker (*arg3*$^+$) was introduced on the left arm of Ch^{16}-MGH at the *yps1*$^+$ locus 84 Kb from the *meu27*$^+$ locus. An additional modification was moving the *MATa* site 33 Kb left of the *ade6-M216* marker. This created Ch^{16}-RMGAH (Figure 2E) [51] which can monitor extensive BIR that results in loss of all markers on the right arm but retention of the *arg3*$^+$ marker. Thus, the *arg3*$^+$ marker distinguishes.

Extensive BIR from chromosome loss. To ensure that the new placement of the *MATa* and *arg3*$^+$ marker on the left arm did not cause a locus-specific form of repair, they generated chromosome Ch^{16}-YAMGH where the *MATa* site was left at the *rad21*$^+$ locus and an *HPH* marker was put 4 Kb from the centromere (Figure 2F). Remarkably, PFGE analysis of the arg+$G418^S$ade-his- or HYG^RG418^Sade-his- colonies showed that the two outcomes were identical suggesting that the mechanism of repair was independent of the break position.

Further analysis showed that following break induction, telomere distal sequences of the break are lost while extensive resection of the centromere proximal sequences occurs. Inverted centromeric repeats facilitate formation of an isochromosome which results from invasion and duplication of both the centromere and the left arm of the chromosome onto the right [51]. Nakamura et al. [33] constructed the ChL mini-chromosome (Figure 2G) to study these isochromosomes and they found that they can occur in the absence of a break. Both groups showed that Rad51 suppresses isochromosome formation [35,51]. Using the ChL chromosome, we have also shown that perturbation of the replication machinery or the centromere heterochromatin increases these isochromosome events. This suggests that isochromosomes originate from improperly repaired random breaks that occur during replication [31]. Remarkably, we also identified some more drastic copy number variations in double chromatin and replication mutants which entirely lost Ch.III and acquired other smaller chromosome fragments. The structure and mechanism of these smaller chromosome fragments remains to be elucidated.

Finally, Ch^{16}-LMYAU was generated to screen Bioneer mutants for chromosome loss phenotypes (Figure 2H) [56]. Previously, the *HO* endonuclease was propagated on a plasmid but here the investigators introduced it at the *yps1*$^+$ locus marked with the *S. cerevisiae LEU2*. The *ura4*$^+$ marker was placed at the *cid2*$^+$ locus. Chromosome loss was assayed by red/white sectoring in response to break induction. Detailed experimental procedures for using these assays were published [57]. Although we do not discuss it here, a chromosome loss assay in diploid cells has also been designed [58]. In addition to chromosome loss, this assay also monitors intra-homologue recombination.

3. Recombination at Repetitive Elements

Another series of assays have been devised in *S. pombe* to study chromosomal recombination at non-tandem repeats (Figure 3). Repetitive elements had been previously shown to cause deletions, inversions or duplications [59,60]. It was known from studies in several species including *S. cerevisiae* that certain genetic mutations act as hotspots for meiotic recombination [61,62]. The *ade6-M26* (G135T) allele in *S. pombe* creates such a hotspot [63]. Remarkably, the *ade6-M375* (G132T) and the *ade6-L469* (C1467T) as well as several other alleles did not serve as recombination hotspots. The G135T, G132T and C1467T mutations inactivate the gene because they introduce stop codons.

Schuchert and Kohli designed a clever non-tandem repeat assay to study crossover frequency at the *ade6-M26* locus (Figure 3A) [64]. They positioned the *ade6-L469* 3′ end mutation on the left side and the *ade6-M26* or *ade6-M375* 5′ end mutation on the right side while placing the functional *ura4*$^+$ gene in between. Then, the investigators assayed for deletion or conversion. Deletion (ade+ura-) can be predicted to arise by several mechanisms. Unequal sister chromatid exchange should generate both

ade-ura+ and ade+ura- phenotypes (Figure 3A(1)). A break between the two *ade6* alleles, followed by resection in both directions past the mutations and annealing can also generate a deletion through SSA (Figure 3A(2)). Since both *ade6* mutations are proximal to the *ura4*$^+$ gene, it is possible to reconstitute a wildtype *ade6*$^+$ allele. Deletion may also occur through an intra-chromosomal crossover and loopout (Figure 3A(3)). An ade+ura+ phenotype arises by replacing the mutation in one allele with the wildtype region of the other allele. The mechanism by which this happened remained elusive until later when the Whitby lab proposed a fork regression and mismatch repair model (see below).

To study mitotic recombination induced by a double strand break the Subramani group introduced the *MATa* site either in the unique sequence between *ura4*$^+$ and *ade6-M26/M375* or within the *ade6-L469* allele (Figure 3B) [65,66]. Upon induction of the DSB, two outcomes predominated (ade+ura- and ade-ura-) which the authors explained to arise by SSA. Subsequent genotyping by restriction digestion or backcrossing identified the exact allele in the ade-ura- phenotypes. ade+ura+ and ade-ura+ recombinants (not shown) also arose at a much lower rate and only when the *HO* restriction site was placed within the *ade6-L469* allele suggesting that the position of the break determines the repair mechanism. These assays were used to analyze the role of several recombination genes in DSB repair [65].

The Whitby lab has subsequently been influential in designing several variations of the tandem repeat assay and have been able to explain some of the more complex outcomes. These assays have been used to identify and characterize genes involved in DNA damage repair [67–78]. The investigators initially designed a system similar to the Schuchert and Kholi assay except that instead of *ura4*$^+$ they placed a *his3*$^+$ marker between the *ade6* alleles (Figure 3C) [79]. This assay was used to show that the ura+his+ recombination outcomes may arise due to recombination dependent restart of stalled replication forks usually through BIR. Inactivation of various cellular processes such as Holliday junction resolution or the checkpoint changes the recombination outcomes [70,79–82]. In a more recent report [83], the Whitby lab introduced a nicking site for the *gpII* M13 phage enzyme. This enzyme makes a nick that is converted to a DSB by the replication fork which approaches from the right (see Figure 3D,E) [84,85]. This assay was used to study restart of stalled replication forks due to the DSB produced by this nick.

To further investigate the effect of replication fork stalling on recombination outcomes, the Whitby lab modified the assay by placing *RTS1*, the naturally occurring replication fork termination site at the mating type loci [86], either between the *his3*$^+$ and the *ade6-M375* alleles or within the *ade6-L469* allele (Figure 3D) [87,88]. *RTS1* is polar meaning that it can only stall forks in one direction, so strains were constructed with different *RTS1* orientations, *RTS1-AO* (active orientation) and *RTS1-IO* (inactive orientation). A cluster of origins of replication are found to the right of the *ade6-M375* allele and the replication fork is predicted to approach from the right (Figure 3E). Two-dimensional gel electrophoresis showed that the *RTS1-AO* efficiently stalls replication forks [89]. The investigators used this assay to study the function of various recombination genes in fork restart and to show that rescue of collapsed replication forks can cause BIR dependent template switching that can generate chromosomal rearrangements. [76,87,88,90,91]. A protocol was published with extensive details on the use of these elegant assays [92].

By inserting the *ade-his-ade* cassette at different distances from the *RTS1* pause site (Figure 3E) the investigators showed that template switching can occur up to 75 Kb from collapsed forks [93]. Collisions between Pol III which transcribes tRNA and replication can cause chromosomal rearrangements [94]. A *tRNA*^{GLU} gene was inserted between the *his3*$^+$ and the *ade6-M375* allele to show that collisions between Pol III and replication machinery increases the frequency of recombination (Figure 3F) [91,93]. An increase in template switching was observed when both *RTS1* and *tRNA*^{GLU} were introduced in the same construct and the orientation of transcription of *tRNA*^{GLU} faced *RTS1* head on [93]. To monitor interaction of fluorescently tagged recombination genes (*rad52*$^+$, *rad51*$^+$, etc.), the *LacO* array was also introduced at different positions within the *ade-his-ade* repeat (Figure 3G) [88,89,95,96].

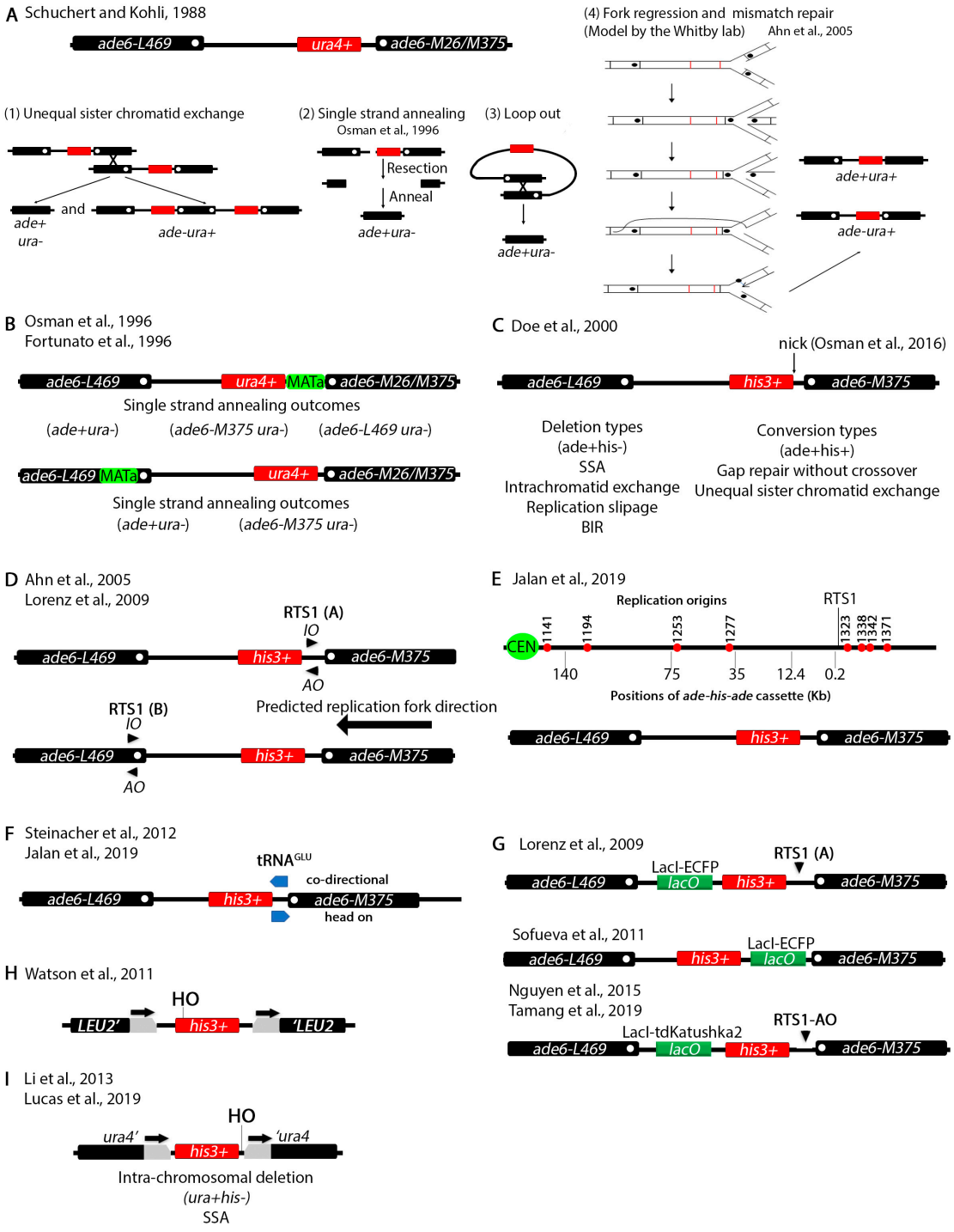

Figure 3. Recombination at tandem repeats. (**A**) An assay to study recombination at non-tandem direct repeats. The *ade6-L469* and *ade6-M26* or *ade6-M375* inactivating alleles were placed on either side of a functional *ura4*$^+$ gene. White dots represent the positions of the mutations in the *ade6* alleles. The strain is adenine auxotrophic and uracil prototrophic (ade-ura+). Different repair pathways lead to various phenotypic outcomes. Unequal sister chromatid exchange (1) produces both ade+ura- and ade-ura+ phenotypes while single strand annealing (2) or loop out (3) produces only ade+ura-. ade+ura+ phenotypes also arose for which the Whitby lab proposed a fork regression and mismatch repair model. (**B**) An assay similar to (**A**) but with the *S. cerevisiae HO* endonuclease restriction site (*MATa*) either between the *ura4*$^+$ and the *ade6-M26/375* alleles or in the *ade6-L469* allele. Shown are phenotypes that

may arise by single strand annealing. (**C**) An assay similar to (**A**) except that *ura4*$^+$ was replaced with *his3*$^+$. The assay was further modified by Osman et al., 2016 to introduce a nick site between the *his3*$^+$ and *ade6-M375* repeat. The nick is created by the M13 bacteriophage *gpII* enzyme. A replication fork which approaches from the right converts this nick into a DSB. (**D**) The assay in (**C**) was modified by introducing the *RTS1* pause site (black arrows) in between the *his3*$^+$ and *ade6-M375* or within the *ade6-L469* allele. Because *RTS1* is polar, two different strains were made for *RTS1*(A) and *RTS1*(B) each with a different orientation AO = active orientation, IO = inactive orientation) of the pause site. (**E**) The *RTS1* was cloned near ori1323 while the *ade-his-ade* cassette was placed at different distances (indicated in kilobases) from the *RTS1*. The relative positions of endogenous replication origins are also shown. (**F**) An assay to test collisions of replication machinery with RNA Pol III. The *tRNA*^{GLU} gene was placed in either of the two orientations between the *his3*$^+$ and the *ade6-M375* allele while the *RTS1* pause site was placed on the right side of *ade6-M375*. (**G**) Three *LacI* arrays using the *ade-his-ade* cassette to allow microscopic visualization of repair dynamics. (**H**) An assay to study single strand annealing. Two *LEU2* fragments with overlapping regions (black arrows) were placed on either side of a functional *his3*$^+$ gene. The *MATa* site was placed on the 5′ end of the *his3*$^+$ gene. (**I**) An assay similar to (**H**) except that *his3*$^+$ is flanked by *ura4* with overlapping regions (arrows) instead of *LEU2*. The *MATa* site was placed on the 3′ end of *his3*$^+$.

An assay to study SSA in *S. pombe* was designed by Watson et al. (Figure 3H) [97]. Two *S. cerevisiae LEU2* fragments with overlapping regions were placed on either side of a functional *his3*$^+$ gene. The MATa sequence was cloned at the 5′ end of *his3*$^+$ right before the start codon. Using this assay, the investigators showed that SSA is *rad52*$^+$ dependent, confirming previous findings. In their report Watson and colleagues also designed an elegant system that allows fast transcriptional induction in *S. pombe*. Historically, transcriptional induction in *S. pombe* relied on the *nmt1* promoter which is repressed by thiamine. Removal of thiamine de-represses the promoter but it takes anywhere between 14–20 h for full induction [98,99]. The new system which is based on upregulation of the *urg1* promoter allows induction within 30 min mirroring the *S. cerevisiae GAL* induction system [100]. The *urg1* system was optimized in a subsequent publication [101]. Other systems for faster induction of gene expression in *S. pombe* that we do not discuss here have also been engineered more recently [102,103].

We also designed an assay to study intrachromosomal deletions at direct repeats (Figure 3I) [31,104]. A functional *his3*$^+$ gene was placed between two truncated *ura4* alleles with 200 bp of overlapping sequence. We showed that this assay can only detect deletions and not conversion.

4. Chromosomal Rearrangements Caused by Stalled or Collapsed Replication Forks at Inverted Repeats

A series of other assays have been designed to study chromosomal rearrangements resulting from stalled replication forks by the Carr, Murray and Lambert labs. Carr and colleagues placed the *RTS1* on either side of *ura4*$^+$ gene on Ch.III (Figure 4A) [105]. Using 2-D gel electrophoresis they showed that these constructs can efficiently stall forks in the vicinity of the *ura4*$^+$ gene. Deletion of several recombination genes including *rad51*$^+$ decreases cell viability suggesting that homologous recombination is required for rescue of stalled forks. PFGE and PCR showed that some of the outcomes resulted in *ura4*$^+$ loss through gene conversion without crossover, while others through a crossover between Ch.III and Ch.II produce a reciprocal translocation (Figure 4B). In all cases, information was exchanged between Ch.III *RTS1* and the endogenous Ch.II *RTS1*. To monitor anaphase bridges by microscopy, the Lambert lab also placed a *LacO* array next to the *RTS1* pause site (Figure 4C) [106].

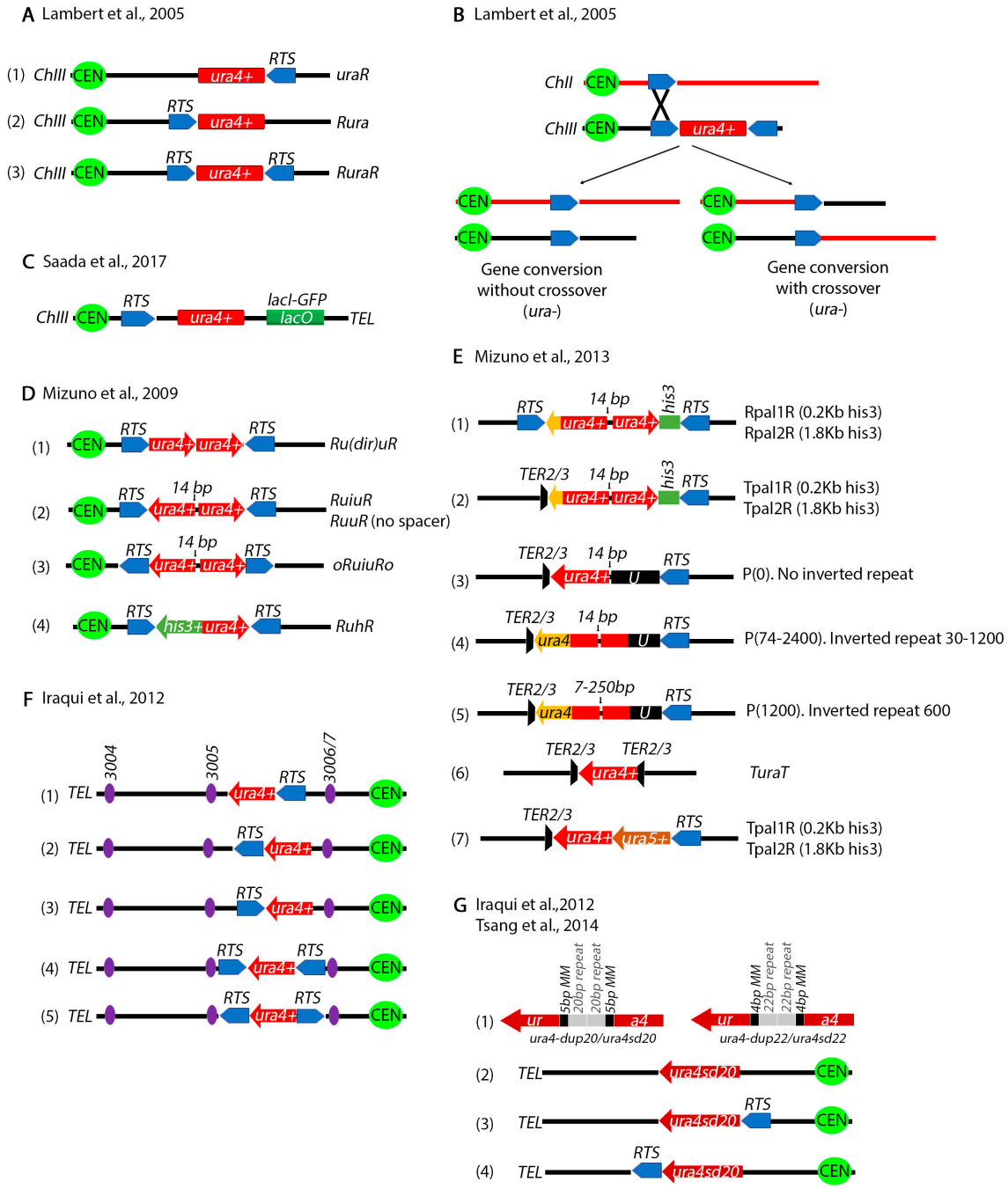

Figure 4. Assays to study gross chromosomal rearrangements at inverted repeats. (**A**) An assay to study fork stalling at repetitive elements. (1) The *RTS1* pause site was placed on the right of a functional *ura4+* gene (*uraR*), (2) left (*Rura*) or (3) both sides (*RuraR*). Fork stalling was assayed using pulse field gel electrophoresis (PFGE). (**B**) Chromosomal rearrangements of constructs in (**A**) can occur by two mechanisms: gene conversion without crossover and gene conversion with crossover. In both cases there is a recombination event between the *RTS1* site next to the *ura4*$^+$ cassette and the endogenous *RTS1* at the *MAT* locus on Ch.II. Both types of events result in loss of *ura4*$^+$. (**C**) Modification of construct in (**A**) to monitor chromosomal dynamics by fluorescence microscopy. A *LacO* array was placed on the telomere side of the *RTS1/ura4*$^+$ cassettes. (**D**) Repetitive elements constructs to study chromosomal rearrangements. (1) *RTS1* cassettes were placed on both sides of two directional *ura4*$^+$ repeats (*Ru(dir)uR*). (2) *RTS1* was placed on both sides of inverted *ura4*$^+$ repeats spaced by 14 bp of unique sequence (*RuiuR*). A construct without the 14bp spacer was also made (*RuuR*) (3) In *oRuiuR* the

RTS1 is in opposite direction from the *RuiuR* construct. (4) In the *RuhR* construct, one of the *ura4*$^+$ repeats was replaced with *his3*$^+$. (**E**) Several constructs to test the effect of repeat length and the position of the replication pause sites in producing rearrangements. (1) Two *ura4*$^+$ inverted repeats spaced by 14 bp of unique sequence were engineered with 0.2 Kb (*Rpal1R*) or 1.8 Kb (*Rpal2R*) *his3*$^+$ sequence between the right *ura4*$^+$ repeat and the *RTS1* pause site. An additional short *ura4*$^+$ was placed between the left *RTS1* and the *ura4*$^+$ repeat (yellow arrow). (2) *Tpal1R* and *Tpal2R* constructs are similar to constructs in (1) except that the left *RTS1* was replaced with three *TER2/3* sequences. (3) In this construct the right *ura4*$^+$ repeat was replaced by a unique sequence. (4) Each of the *ura4*$^+$ repeat sizes were varied between 30–1200 base pairs. (5) The spacer between the inverted repeats was varied between 7–250 base pairs. (6) *ura4*$^+$ cassette flanked by the *TER2/3* termination sites. (7). Direct repeats but one of the *ura4*$^+$ repeats was replaced with a *ura5*$^+$ repeat. (**F**) The *ura4*$^+$ and *RTS1* pause sites were placed next to known origins of replication (3004, 3005, 3006/7). (1) Co-directional *ura4*$^+$ and *RTS1* with *RTS1* placed either after (1) or in front (2) of the *ura4*$^+$ repeat. (3) Construct similar to (**A**) (2) and (4) construct similar to (**A**) (3) placed between the 3005 and 3006/7 replication origins. (5) Construct similar to (4) but with *RTS1* in the opposite orientation. (**G**) Constructs to test microhomology mediate repair caused by rescued replication forks. (1) Two different microhomology constructs. *ura4-dup20/ura4sd20* was engineered by placing two 20 bp (grey boxes) repeats flanked by 5 bp of microhomology sequences (black boxes) in the middle of the *ura4*$^+$ gene. *ura4-dup22/ura4sd22* is has 22 bp repeats flanked by 4 bp of homology. Microhomology mediated repair was investigated either in the absence of a pause site (2) or with the pause site placed on the left (3) or right (4) of the construct. Only *ura4sd20* is shown.

Mizuno et al. engineered several repeat constructs flanked by *RTS1* sites (Figure 4D) [107]. Using these constructs, the investigators showed that recombination dependent rescue of stalled replication forks at inverted repeats can produce dicentric and acentric isochromosomes. In subsequent and even more sophisticated studies, the investigators generated a series of more complex constructs to precisely analyze the mechanisms of chromosomal rearrangements at inverted repeats (Figure 4E) [108]. The length of the repeats as well as the gap between the repeats was varied, unique sequences were introduced at either side of the repeats, *RTS1* sites were placed at different distances from the repeats and the *TER2/3* ribosomal fork barrier was also tested. Their findings showed that inverted repeats cause forks to turn around or "execute a U-turn" and generate gross chromosomal rearrangements. Remarkably, the DNA damage checkpoint does not appear to detect the recombination intermediates that cause these rearrangements, at least in the cell cycle in which they occur [109].

The position of the *RTS1* was varied relative to several Ch.III replication origions (Figure 4F) [110,111] to show that when a replication fork approaching from one of these origins collides with the *RTS1* site, it causes deletions in addition to gross chromosomal translocations. To test for replication fork slippage, the investigators designed a construct where the *ura4*$^+$ gene was interrupted by 20 bp repeats flanked by 5 bp of microhomology sequences (Figure 4G) [77,110]. A slightly modified construct has 22 bp repeats flanked by 4 bp of microhomology (Figure 4G). Both constructs inactivate the *ura4*$^+$ gene. Microhomology mediated repair results in a functional *ura4*$^+$. Using these constructs, it was shown that fork slippage, but not translesion synthesis or mismatch repair, is responsible for the restoration of the functional *ura4*$^+$ cassette. The intra-S phase DNA damage checkpoint (Rad3) represses fork slippage and microhomology mediated repair at stalled forks [77]. Further, the NHEJ factor Ku appears to regulate recombination at arrested forks by controlling end resection [112].

5. Mating Type Loci Serve as a Natural Site for Studying Collapsed Replication Forks

The mating type of a *S. pombe* cell is determined by the allele present at the *mat1* cassette (Figure 5A) [113]. This allele can be either *mat1M* (M cell, M stands for minus) or *mat1P* (P cell, P stands for plus) [114,115]. Switching between *mat1M* and *mat1P* is accomplished by copying information from the silent *mat2-P* and *mat3-M* cassettes [116–119]. In addition to the allele present at the *mat1* locus, the mating type of a population of cells is also determined by the ability to switch and the alleles present at the silent *mat2-P* and *mat3-M* regions. Wild type h^{90} cells can switch information at the *mat1* locus and

are mixture of M and P cells [120–123]. A population that has the M allele at the *mat1* locus (*mat1M*) and lost the ability to switch is h^-. A population may also be h^- if it lost the *mat2-P* locus and repairs the *mat1M* with the same information (e.g., from *mat3-M*). Alternatively, a population of cells are h^+ if the P allele is expressed from the *mat1* locus (*mat1P*) and the strain is unable to switch (e.g., *mat1PΔ17*).

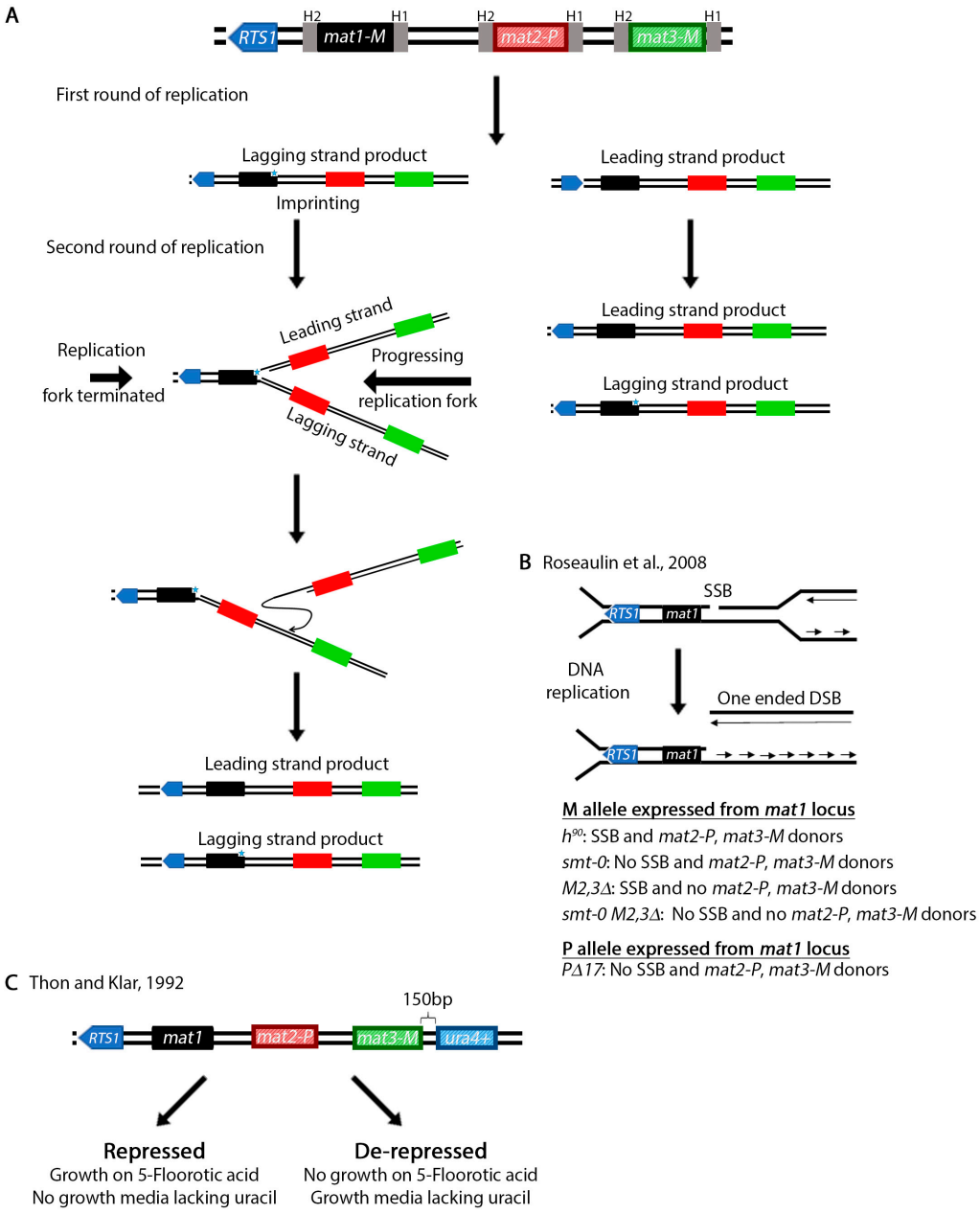

Figure 5. Mating type switching in *S. pombe*. (**A**) Diagram of the process of mating type switching. The mating type region has three cassettes *mat1*, *mat2-P(plus)* and *mat3-M(minus)*. Only *mat1* is expressed with either P or M while *mat2-P* and *mat3-M* are silenced. The shading of *mat2-P* and *mat3-M* diagrams represents this silencing. Information switches from *mat2-P* and *mat3-M* onto *mat1* so that *mat1* expresses either P or M. All three cassettes are flanked by homologous regions (H1, H2) that facilitate recombination. In this diagram, we begin with a hypothetical example where *mat1* expresses the *M* information. After one round of replication, an imprint consisting of insertion of one or two ribonucleotides or a single strand nick is made next to the *mat1-M* cassette on the lagging strand (blue star). For simplicity, the top diagram does not have the imprint. In the second round of replication, the

leading strand collides with the imprint and produces a blunt one-ended DSB. To ensure that only the leading strand passes through the imprint, the replication fork from the other direction is paused and terminated by the *RTS1* site. The one-ended break is repaired by copying information from the *mat2-P* or *mat3-M* regions. Since in our example the *M* information was expressed at *mat1*, the break may be repaired using *mat2-P* and the information at *mat1* switches. Note that the imprint is always placed on the lagging strand with each DNA replication. (**B**) Exploiting the mating type loci to study rescue of collapsed forks. Collision of the leading strand with the imprint produces a blunt one-ended break that can be studied in WT and other control strains. h^{90} is a wild type strain capable of switching that represents a mix of M and P cells. The *smt-0* has a deletion that eliminates the imprint while *M2,3*Δ have deletions in the *mat2-M* and *mat3-P* regions. *smt-0 M2,3*Δ is a double mutant. The *P*Δ*17* mutant is similar to *smt-0* except that in this strain the *mat1* locus expresses the *P* information. (**C**) An assay to study silencing at the mating type loci. The functional $ura4^+$ gene was places 150 base pairs from *mat3-M*. If repressed, the strain can grow on 5-fluoroorotic acid (5-FOA) which negatively selects against uracil prototrophs and die on minimal media lacking uracil. If de-repressed, the strain will die on 5-FOA and grow on minimal media lacking uracil.

In wild type populations, switching occurs in only 25% of the cells [124]. This is because unlike in *S. cerevisiae* where switching is initiated by a double strand break generated by the *HO* endonuclease [125], in *S. pombe* switching begins with an imprint in the lagging strand during an initial round of DNA replication. Two concurrent models exist to explain the nature of the imprint. The imprint may be caused by the introduction of one or two ribonuclotides in the DNA sequence [126–128] or the generation of a single strand break [129] or possibly both at the same time. Regardless, the imprint is converted to a one-ended double strand break in the next round of replication [129–133]. However, only one of the replication forks may convert the imprint into a DSB. To ensure that the other replication fork does not pass through the imprint, replication is terminated by the above mentioned *RTS1* site [86,134]. This process allows unidirectional transfer of information from the two *mat2-P* and *mat3-M* cassettes onto *mat1* in only one of the four cells.

Investigation of the mating type loci in *S. pombe*, which increased our understanding of replication, recombination and gene silencing has been reviewed previously [120,135]. This natural system is a remarkable assay for the study of the role of DNA recombination in restart of collapsed replication forks. Perhaps even more important is the fact that the system produces one-ended DSBs which more accurately resemble the type of substrates resulting from collapsed replication forks [136]. Using wild type cells or several mating type defective mutants (Figure 5B) [130,137,138] the role of various DNA damage response genes have been investigated [136,139,140]. Work has also led to the identification of several recombination and replication genes, particularly the *swi* (switching) genes [117,118,141,142]. Additionally, various mechanisms of gene silencing were identified (reviewed in reference [143]). For example, unlike the centromeres, the mating type loci are silenced through an RNAi independent mechanism [144–146]. Work on silencing led to the identification of the *clr* (cryptic loci regulator) genes [147–149]. To investigate silencing, Thon and Klar placed the $ura4^+$ gene 150 bp from the *mat3* cassette [147] (Figure 5C). Finally, as Klar et al. point out in their review [135], the asymmetric mating type switching in *S. pombe* may also explain how genes are differentially regulated during development of higher eukaryotic organisms.

6. Other Fluorescence and Biochemical Assays

To investigate centromere dynamics, Nabeshima et al. placed a *LacO* array at the $lys1^+$ locus, 30 Kb from the centromere (Figure 6A) [150]. The Russell lab modified this assay by placing the *HO* endonuclease restriction site 1.5 Mb away at the $arg3^+$ locus within 2.8 Kb of the *LacO* array (Figure 6B) [151]. Using these assays, they showed that Crb2-YFP (yellow fluorescent protein) co-localizes with the *LacI-GFP* (green fluorescent protein) bound to the *LacO* array suggesting that Crb2 interacts with the chromosome at the site of the DSB. When the break was at the $arg3^+$ locus, no co-localization was observed because the Crb2-YFP interacts with a DNA sequence too far from

the *LacO* array. Several other constructs were made without the *LacO* array to investigate foci of various fluorescent-tagged proteins in response to a DSB (Figure 6B). For finer analysis of repair proteins interacting with the break, the investigators next turned to Chromatin IP. Primers were designed to amplify sequences by PCR at 0.2, 2.0, 9.0 and 16.0 Kb and the interaction of a variety of proteins with the break were tested biochemically (Figure 6C) [152,153]. Using these assays, the investigators have unraveled the role of various DNA damage checkpoint and repair proteins in processing of DSBs [136,152,154–160]. Not discussed here are some other biochemical assays that the Russell lab engineered, including some assays to study resection [161] with some adaptations from *S. cerevisiae* [162].

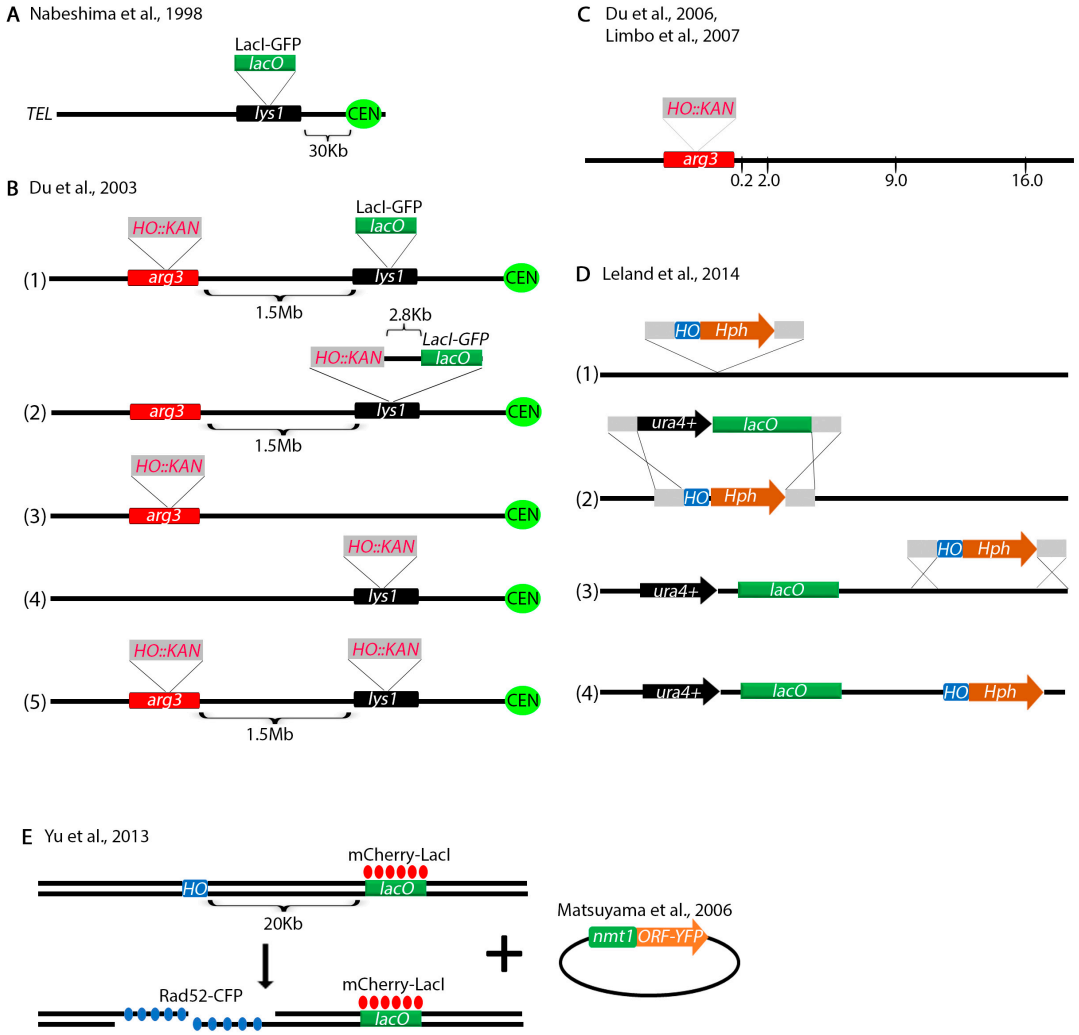

Figure 6. Fluorescence and biochemical assays. (**A**) An assay designed by Nabeshima et al. to study centromere dynamics. A *LacO* array was placed 30 Kb from the centromere of Ch.I. *LacI-GFP* binding allows visualization of centromeres. (**B**) Assays developed by Du et al. to study repair of a DSB. (1) The *HO* endonuclease restriction site marked with *KAN* was placed 1.5 Mb away from the *LacO* array at the *arg3*$^+$ locus. (2) *HO::KAN* was placed 2.8 Kb from the *LacO* array. Constructs without a *LacO* array with the *HO* restriction site at *arg3*$^+$ (3), *lys1*$^+$ (4) or both *arg3*$^+$ and *lys1*$^+$ (5) were also engineered. These constructs can be used to study foci of fluorescently tagged DNA damage repair proteins. (**C**) The construct in (**B**) (3) was adapted for Chromatin Immunoprecipitation. PCR primers were engineered at 0.2, 2.0, 9.0 and 16.0 Kb from the break. Upon induction of the break, multiplex PCR can analyze binding of various proteins at all four locations at once. (**D**) An assay to integrate the *LacO* array and

the *HO* restriction site anywhere in the yeast genome. Please see text for details. (**E**) An assay to study YFP tagged proteins interacting with a DSB. A *lacO* array that interacts with LacI-mCherry was placed 30 Kb from the *HO* endonuclease restriction site. The strain also contains Rad52 fused with cyan fluorescent protein (Rad52-CFP). A library of YFP tagged proteins was transformed in the cells and colocalization of all three foci (red, blue, yellow) was monitored.

Another ingenious assay was designed by Leland and King to introduce a *LacO* array and the *HO* restriction site anywhere in the genome (Figure 6D) [163]. This technique requires several steps. First, the *HO* restriction site marked with the *HPH* marker and flanked by two homology regions is placed at a desired location in the genome (Figure 6D(1)). Then, a sequence harboring the *LacO* array marked with *ura4*$^+$ and flanked by the same homologous sequences as the *HO* restriction site is integrated at the *HO* locus (Figure 6D(2)). The *HO* restriction site is re-integrated at a location neighboring the *LacO* array (Figure 6D(3)). This produces a construct with an *HO* restriction site next to the *LacO* array (Figure 6C(4)) similar to the Du et al. assay (Figure 6B). The advantage of this technique is that the *LacO* and the *HO* restriction site can be introduced anywhere in the genome.

Yu et al. has designed an assay to screen for proteins interacting with a DSB (Figure 6E) [164]. They engineered the *HO* endonuclease restriction site 20 Kb from a *LacO* array that binds LacI-Cherry. The strain also expresses Rad52-CFP (cyan fluorescent protein) which interacts with DSBs. Upon DSB induction, co-localization of red and blue foci indicates that Rad52-CFP interacted with the DSB. When they transformed a library of *S. pombe* YFP tagged proteins [165], they were able to screen for other proteins that interact with the DSB by monitoring co-localization of all three foci (red, blue, yellow).

7. Non-Homologous Repair

Non-homologous repair can occur in the absence of homologous regions. Several assays have been designed to test non-homologous repair in *S. pombe*. In an NHEJ assay designed by Goedecke and colleagues, a plasmid is linearized with various restriction sites to produce non-homologous ends (Figure 7A) [166]. The restriction sites used to generate one of the ends are different from those used to generate the other end, thus ensuring that the ends cannot be re-ligated. The linear fragment is transformed into living cells and allowed to re-circularize. The junction is amplified by PCR and sequenced. Using this assay, the investigators showed that the ends are resected up to 14 bps prior to rejoining. A similar assay by Manolis et al. relies on transforming linearized sequences with just one restriction enzyme (*Pvu*II) (Figure 7B) [167]. Subsequent sequence analysis of rejoined products identified various sequence alterations at the junction. The investigators also showed that in *S. pombe* *rad50*$^+$, *mre11*$^+$ and the DNA damage checkpoint is not required for NHEJ. These plasmid type NHEJ assays were instrumental in demonstrating that key components of NHEJ are conserved form yeast to humans [168,169].

In a variation of these assays, Anabelle Decottignies used PCR to amplify a linear fragment (Figure 7C) [170]. The fragment was transformed and allowed to re-circularize in living cells followed by junction analysis. Remarkably, she identified mitochondrial DNA sequences at the junctions. As she points out, the advantage of this assay is that primers with different microhomology overhangs can be engineered to test recircularization of different ends. This assay was successfully used by the Du lab to identify the XRCC4 NHEJ protein in a genome wide screen [171]. The Du lab also designed an assay that relies on the *HO* restriction enzyme (Figure 7D) [172] similarly to their previous assays (Figure 6B). In this assay, the 24 base pair *HO* restriction site marked with the *natMX* cassette (*nat* confers resistance to nourseothricin) was cloned at the *arg3*$^+$ locus on Ch.I. The *nmt1-HO* endonuclease was integrated at *ars1*$^+$. Because the cells were grown under continuous expression of the *HO* endonuclease (no thiamine in the media), only those cells with imprecise repair of the junction (either deletions or insertions) could survive. These cells had destroyed the *HO* endonuclease restriction site, in effect inactivating the function of the enzyme. The junction of surviving cells was amplified by PCR and sequenced either by

the Sanger methods or by Illumina sequencing. This assay is a useful tool for studying break repair that does not rely on homologous recombination.

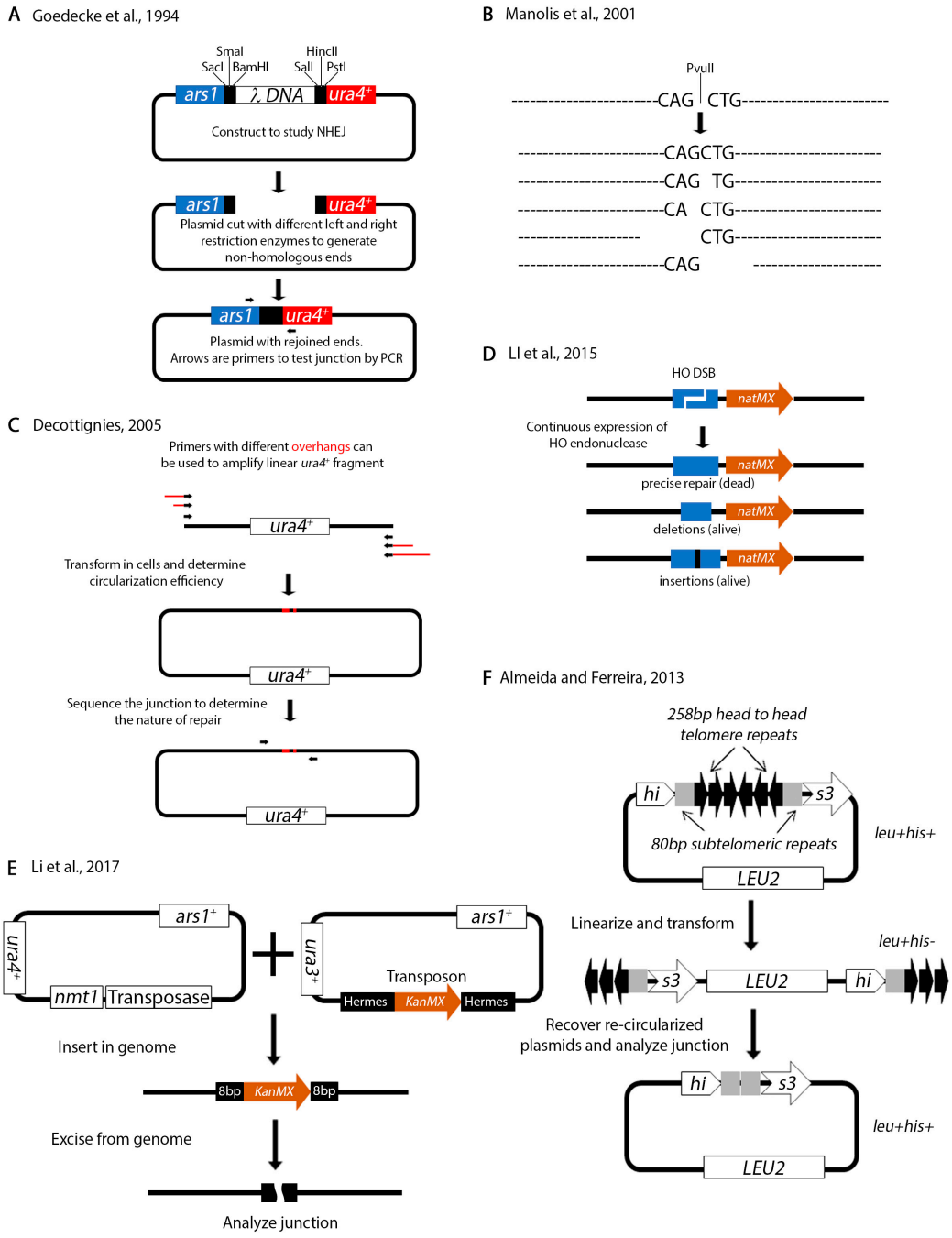

Figure 7. Assays to test non-homologous repair. (**A**) A plasmid-based assay to study non-homologous end joining. A λ DNA fragment is flanked by three unique restriction sites on each side. The plasmid is cut with different left and right restriction enzymes then transformed as a linear fragment into cells. Propagation of the transformed fragment in cells is only possible upon re-ligation of linear fragment ends. Thus, transformation frequency can be used as an indicator of repair efficiency. PCR across the junction (black arrows represent primers) followed by sequencing can determine the ligation patterns. (**B**) An assay similar to (**A**) except that the plasmid is cut with only one enzyme (*Pvu*II). After relegation, the junction is analyzed for reconstitution of the *Pvu*II restriction site or deletion and insertion of various

nucleotides. (**C**) In this assay, PCR primers (black arrows) can be designed with various sequence overhangs (red lines). Linear fragments are amplified and transformed in yeast. Repair is analyzed as in (**A**). (**D**) The *HO* restriction site marked with *nat*MX was cloned at the *arg1*$^+$ locus on Ch.I. Continuous expression of *HO* endonuclease will kill all cells that do not repair the break or repair it correctly because it reconstitutes the restriction site and are vulnerable to re-cutting. Incorrect repair destroys the restriction site and allows cells to live. The authors used both Sanger sequencing and Illumina next generation sequencing to analyze the junction. (**E**) A transposon-based assay to study genome integration and excision. A plasmid encoding the transposase is co-transformed with another plasmid with transposon integration sequences (Hermes) flanking a KanMX cassette. De-repression of the transposase allows integration of the KanMX cassette randomly in the genome. Following integration, re-expression of the transposase will cause excision of the transposon. Analysis of the junction sequences can determine the form of repair. (**F**) An assay to test the role of telomeres in preventing chromosome end fusions. Two head to head telomeric repeats were cloned in the second intron of the *his3*$^+$ gene. Each repeat also contains 80 bp of subtelomeric sequences. This telomere repeat interruption does not disrupt transcription of the *his3*$^+$ gene. Consequently, the plasmid is his+leu+. The plasmid is linearized (destroying transcription of *his3*$^+$) between the telomeric repeats and introduced into cells. Because each end is capped by telomeres, the fragment can be maintained as a mini-chromosome, which is leu+his-. Deletion of telomerase causes telomere attrition and fusion of the ends which reconstitutes the *his3*$^+$ gene. Such fusions can be selected for on media lacking both histidine and leucine. Analysis of the fusion junction can determine the precision of repair.

A different NHEJ assay was designed by Li et al. that relies on analyzing the genome insertion and excision of a transposon (Figure 7E) [173]. Two plasmids, one encoding the transposase and the other the transposon are co-transformed in the cells. De-repression of the transposase causes random insertion of the transposon. The role of NHEJ factors can be investigated by monitoring the efficiency of insertion. Alternatively, re-expression of the transposase will cause excision of the transposon from the genome. The transposon is characterized by 8 bp of homology on either end. Analysis of the repaired junction can determine the nature of the microhomology mediated repair.

Finally, we want to mention an assay to study chromosome end fusions due to telomere erosion (Figure 7F) [174]. The *his3*$^+$ is one of the genes in *S. pombe* that has introns. The investigators introduced head to head telomeric repeats in the second intron of *his3*$^+$. This insertion does not affect the function of *his3*$^+$. The plasmid is linearized between the telomeric repeats and transformed into living cells. The construct may be propagated as a linear fragment because it has telomeres and can be selected for on media lacking leucine. However, the linear fragment interrupts transcription of the *his3*$^+$ gene. Deletion of telomerase causes telomere attrition and re-circularization of the fragment which can be selected for on media lacking histidine because it reconstitutes the function of the *his3*$^+$ gene. The plasmid can be recovered and the junction analyzed by sequencing.

8. Concluding Remarks

Although none of the assays mentioned here can independently unravel the function of every repair pathway, when the data are put together, a clearer picture emerges. This is particularly true if combined with results from other systems such as *S. cerevisiae*. Nevertheless, the work done in *S. pombe* has not just been complementary to the work done in other model systems but instrumental in discovering and defining new mechanisms of DSB repair.

Nevertheless, there are many unanswered questions that remain. For example, the role of chromatin remodeling in modulating DSB repair requires further investigation. The fact that histone modifications play a role in biasing repair towards different pathways is clear. However, how these modifications choreograph repair is not well understood [175]. This is because histone modifications are transient and hard to capture. Experiments using some of the assays described here that either knock out histone modifying enzymes or substitute modifiable histone residues for unmodifiable ones have provided some insight but these are likely to cause genome wide changes which complicates

interpretation. Some recent experiments have also shown that RNA plays a major role in DSB repair [176] but the exact dynamics are poorly understood. With advances in technology, such as CRISPR, it is almost certain that in the next few years we will see much more complex assays that are likely to elucidate some of these questions.

Author Contributions: H.M.H. and B.E.L. performed an extensive literature search, summarized the papers read and made some figures. R.C.P. wrote the first draft. H.M.H. and B.E.L. revised the draft. All authors contributed equally to the revisions to address referees' points. All authors have read and agreed to the published version of the manuscript.

Funding: This work was supported in part by the National Institutes of Health (grant number RO3 CA223545-01). Other support to RCP from The Ohio State University James Comprehensive Cancer Center. Bailey E. Lucas was supported in part by an Ohio State University Comprehensive Cancer Center Pelotonia Undergraduate Fellowship.

Acknowledgments: We thank James and Ellen Bazzoli for their generous donation to sponsor our laboratory.

Conflicts of Interest: The authors declare no conflict of interest.

References

1. Kerzendorfer, C.; O'Driscoll, M. Human DNA damage response and repair deficiency syndromes: Linking genomic instability and cell cycle checkpoint proficiency. *DNA Repair* **2009**, *8*, 1139–1152. [CrossRef]
2. White, R.R.; Vijg, J. Do DNA Double-Strand Breaks Drive Aging? *Mol. Cell* **2016**, *63*, 729–738. [CrossRef]
3. Jeggo, P.A.; Lobrich, M. How cancer cells hijack DNA double-strand break repair pathways to gain genomic instability. *Biochem. J.* **2015**, *471*, 1–11. [CrossRef] [PubMed]
4. Janssen, A.; van der Burg, M.; Szuhai, K.; Kops, G.J.; Medema, R.H. Chromosome segregation errors as a cause of DNA damage and structural chromosome aberrations. *Science* **2011**, *333*, 1895–1898. [CrossRef] [PubMed]
5. Lasko, D.; Cavenee, W.; Nordenskjold, M. Loss of constitutional heterozygosity in human cancer. *Annu. Rev. Genet.* **1991**, *25*, 281–314. [CrossRef] [PubMed]
6. Ortega, V.; Chaubey, A.; Mendiola, C.; Ehman, W., Jr.; Vadlamudi, K.; Dupont, B.; Velagaleti, G. Complex Chromosomal Rearrangements in B-Cell Lymphoma: Evidence of Chromoanagenesis? A Case Report. *Neoplasia* **2016**, *18*, 223–228. [CrossRef] [PubMed]
7. Mehta, A.; Haber, J.E. Sources of DNA double-strand breaks and models of recombinational DNA repair. *Cold Spring Harb. Perspect. Biol.* **2014**, *6*, a016428. [CrossRef]
8. Nikolov, I.; Taddei, A. Linking replication stress with heterochromatin formation. *Chromosoma* **2016**, *125*, 523–533. [CrossRef]
9. Tabancay, A.P., Jr.; Forsburg, S.L. Eukaryotic DNA replication in a chromatin context. *Curr. Top. Dev. Biol.* **2006**, *76*, 129–184. [CrossRef]
10. Prado, F.; Aguilera, A. Impairment of replication fork progression mediates RNA polII transcription-associated recombination. *EMBO J.* **2005**, *24*, 1267–1276. [CrossRef]
11. Kaushal, S.; Freudenreich, C.H. The role of fork stalling and DNA structures in causing chromosome fragility. *Genes Chromosomes Cancer* **2019**, *58*, 270–283. [CrossRef] [PubMed]
12. Irony-Tur Sinai, M.; Kerem, B. Genomic instability in fragile sites-still adding the pieces. *Genes Chromosomes Cancer* **2019**, *58*, 295–304. [CrossRef]
13. Cavalier-Smith, T. Origins of the machinery of recombination and sex. *Heredity* **2002**, *88*, 125–141. [CrossRef] [PubMed]
14. Piazza, A.; Heyer, W.D. Homologous Recombination and the Formation of Complex Genomic Rearrangements. *Trends. Cell. Biol.* **2019**, *29*, 135–149. [CrossRef]
15. West, S.C.; Blanco, M.G.; Chan, Y.W.; Matos, J.; Sarbajna, S.; Wyatt, H.D. Resolution of Recombination Intermediates: Mechanisms and Regulation. *Cold Spring Harb. Symp. Quant. Biol.* **2015**, *80*, 103–109. [CrossRef] [PubMed]
16. Prado, F. Homologous recombination maintenance of genome integrity during DNA damage tolerance. *Mol. Cell. Oncol.* **2014**, *1*, e957039. [CrossRef] [PubMed]
17. San Filippo, J.; Sung, P.; Klein, H. Mechanism of eukaryotic homologous recombination. *Annu. Rev. Biochem.* **2008**, *77*, 229–257. [CrossRef]

18. Ait Saada, A.; Lambert, S.A.E.; Carr, A.M. Preserving replication fork integrity and competence via the homologous recombination pathway. *DNA Repair* **2018**, *71*, 135–147. [CrossRef]
19. Daley, J.M.; Kwon, Y.; Niu, H.; Sung, P. Investigations of homologous recombination pathways and their regulation. *Yale J. Biol. Med.* **2013**, *86*, 453–461.
20. Pannunzio, N.R.; Li, S.; Watanabe, G.; Lieber, M.R. Non-homologous end joining often uses microhomology: Implications for alternative end joining. *DNA Repair* **2014**, *17*, 74–80. [CrossRef]
21. Malkova, A.; Haber, J.E. Mutations arising during repair of chromosome breaks. *Annu. Rev. Genet.* **2012**, *46*, 455–473. [CrossRef] [PubMed]
22. Hedges, S.B. The origin and evolution of model organisms. *Nat. Rev. Genet.* **2002**, *3*, 838–849. [CrossRef] [PubMed]
23. Heckman, D.S.; Geiser, D.M.; Eidell, B.R.; Stauffer, R.L.; Kardos, N.L.; Hedges, S.B. Molecular evidence for the early colonization of land by fungi and plants. *Science* **2001**, *293*, 1129–1133. [CrossRef] [PubMed]
24. Wood, V.; Gwilliam, R.; Rajandream, M.A.; Lyne, M.; Lyne, R.; Stewart, A.; Sgouros, J.; Peat, N.; Hayles, J.; Baker, S.; et al. The genome sequence of Schizosaccharomyces pombe. *Nature* **2002**, *415*, 871–880. [CrossRef]
25. Rubin, G.M.; Yandell, M.D.; Wortman, J.R.; Gabor Miklos, G.L.; Nelson, C.R.; Hariharan, I.K.; Fortini, M.E.; Li, P.W.; Apweiler, R.; Fleischmann, W.; et al. Comparative genomics of the eukaryotes. *Science* **2000**, *287*, 2204–2215. [CrossRef]
26. Forsburg, S.L. The yeasts Saccharomyces cerevisiae and Schizosaccharomyces pombe: Models for cell biology research. *Gravit. Space Biol. Bull.* **2005**, *18*, 3–9.
27. Halazonetis, T.D.; Gorgoulis, V.G.; Bartek, J. An oncogene-induced DNA damage model for cancer development. *Science* **2008**, *319*, 1352–1355. [CrossRef]
28. Branzei, D.; Foiani, M. Maintaining genome stability at the replication fork. *Nat. Rev. Mol. Cell Biol.* **2010**, *11*, 208–219. [CrossRef]
29. Madireddy, A.; Gerhardt, J. Replication Through Repetitive DNA Elements and Their Role in Human Diseases. *DNA Replication Old Princ. New Discov.* **2017**, *1042*, 549–581. [CrossRef]
30. Forsburg, S.L. The CINs of the centromere. *Biochem. Soc. Trans.* **2013**, *41*, 1706–1711. [CrossRef]
31. Li, P.C.; Petreaca, R.C.; Jensen, A.; Yuan, J.P.; Green, M.D.; Forsburg, S.L. Replication fork stability is essential for the maintenance of centromere integrity in the absence of heterochromatin. *Cell Rep.* **2013**, *3*, 638–645. [CrossRef] [PubMed]
32. Onaka, A.T.; Toyofuku, N.; Inoue, T.; Okita, A.K.; Sagawa, M.; Su, J.; Shitanda, T.; Matsuyama, R.; Zafar, F.; Takahashi, T.S.; et al. Rad51 and Rad54 promote noncrossover recombination between centromere repeats on the same chromatid to prevent isochromosome formation. *Nucleic Acids Res.* **2016**, *44*, 10744–10757. [CrossRef] [PubMed]
33. Nakamura, K.; Okamoto, A.; Katou, Y.; Yadani, C.; Shitanda, T.; Kaweeteerawat, C.; Takahashi, T.S.; Itoh, T.; Shirahige, K.; Masukata, H.; et al. Rad51 suppresses gross chromosomal rearrangement at centromere in Schizosaccharomyces pombe. *EMBO J.* **2008**, *27*, 3036–3046. [CrossRef]
34. Forsburg, S.L.; Shen, K.F. Centromere Stability: The Replication Connection. *Genes-Basel* **2017**, *8*. [CrossRef]
35. He, H.J.; Gonzalez, M.; Zhang, F.; Li, F. DNA replication components as regulators of epigenetic inheritance-lesson from fission yeast centromere. *Protein Cell* **2014**, *5*, 411–419. [CrossRef]
36. Mizuguchi, T.; Barrowman, J.; Grewal, S.I.S. Chromosome domain architecture and dynamic organization of the fission yeast genome. *Febs Lett.* **2015**, *589*, 2975–2986. [CrossRef]
37. Forsburg, S.L. The art and design of genetic screens: Yeast. *Nat. Rev. Genet.* **2001**, *2*, 659–668. [CrossRef] [PubMed]
38. Li, J.; Sun, H.; Huang, Y.; Wang, Y.; Liu, Y.; Chen, X. Pathways and assays for DNA double-strand break repair by homologous recombination. *Acta Biochim. Biophys. Sin.* **2019**, *51*, 879–889. [CrossRef] [PubMed]
39. Klein, H.L.; Bacinskaja, G.; Che, J.; Cheblal, A.; Elango, R.; Epshtein, A.; Fitzgerald, D.M.; Gomez-Gonzalez, B.; Khan, S.R.; Kumar, S.; et al. Guidelines for DNA recombination and repair studies: Cellular assays of DNA repair pathways. *Microb. Cell* **2019**, *6*, 1–64. [CrossRef] [PubMed]
40. Klein, H.L.; Ang, K.K.H.; Arkin, M.R.; Beckwitt, E.C.; Chang, Y.H.; Fan, J.; Kwon, Y.; Morten, M.J.; Mukherjee, S.; Pambos, O.J.; et al. Guidelines for DNA recombination and repair studies: Mechanistic assays of DNA repair processes. *Microb. Cell* **2019**, *6*, 65–101. [CrossRef]
41. Kai, M.; Taricani, L.; Wang, T.S. Methods for studying mutagenesis and checkpoints in Schizosaccharomyces pombe. *Methods Enzymol.* **2006**, *409*, 183–194. [CrossRef] [PubMed]

42. Niwa, O.; Matsumoto, T.; Yanagida, M. Construction of a Minichromosome by Deletion and Its Mitotic and Meiotic Behavior in Fission Yeast. *Mol. Gen. Genet.* **1986**, *203*, 397–405. [CrossRef]
43. Niwa, O.; Matsumoto, T.; Chikashige, Y.; Yanagida, M. Characterization of Schizosaccharomyces pombe minichromosome deletion derivatives and a functional allocation of their centromere. *EMBO J.* **1989**, *8*, 3045–3052. [CrossRef] [PubMed]
44. Bloom, K.; Costanzo, V. Centromere Structure and Function. *Prog. Mol. Subcell. Biol.* **2017**, *56*, 515–539. [CrossRef]
45. Kohli, J.; Hottinger, H.; Munz, P.; Strauss, A.; Thuriaux, P. Genetic-Mapping in Schizosaccharomyces-Pombe by Mitotic and Meiotic Analysis and Induced Haploidization. *Genetics* **1977**, *87*, 471–489.
46. Steiner, N.C.; Hahnenberger, K.M.; Clarke, L. Centromeres of the Fission Yeast Schizosaccharomyces-Pombe Are Highly Variable Genetic-Loci. *Mol. Cell. Biol.* **1993**, *13*, 4578–4587. [CrossRef]
47. Gygax, A.; Thuriaux, P. A Revised Chromosome Map of the Fission Yeast Schizosaccharomyces-Pombe. *Curr. Genet.* **1984**, *8*, 85–92. [CrossRef]
48. Murakami, S.; Matsumoto, T.; Niwa, O.; Yanagida, M. Structure of the fission yeast centromere cen3: Direct analysis of the reiterated inverted region. *Chromosoma* **1991**, *101*, 214–221. [CrossRef]
49. Lock, A.; Rutherford, K.; Harris, M.A.; Wood, V. PomBase: The Scientific Resource for Fission Yeast. *Eukaryot. Genom. Databases Methods Protoc.* **2018**, *1757*, 49–68. [CrossRef]
50. PomBase. The Scientific Resource for Fission Yeast. Available online: https://www.pombase.org/ (accessed on 15 December 2019).
51. Tinline-Purvis, H.; Savory, A.P.; Cullen, J.K.; Dave, A.; Moss, J.; Bridge, W.L.; Marguerat, S.; Bahler, J.; Ragoussis, J.; Mott, R.; et al. Failed gene conversion leads to extensive end processing and chromosomal rearrangements in fission yeast. *EMBO J.* **2009**, *28*, 3400–3412. [CrossRef]
52. Cromie, G.A.; Rubio, C.A.; Hyppa, R.W.; Smith, G.R. A natural meiotic DNA break site in Schizosaccharomyces pombe is a hotspot of gene conversion, highly associated with crossing over. *Genetics* **2005**, *169*, 595–605. [CrossRef] [PubMed]
53. Cullen, J.K.; Hussey, S.P.; Walker, C.; Prudden, J.; Wee, B.Y.; Dave, A.; Findlay, J.S.; Savory, A.P.; Humphrey, T.C. Break-induced loss of heterozygosity in fission yeast: Dual roles for homologous recombination in promoting translocations and preventing de novo telomere addition. *Mol. Cell. Biol.* **2007**, *27*, 7745–7757. [CrossRef] [PubMed]
54. Prudden, J.; Evans, J.S.; Hussey, S.P.; Deans, B.; O'Neill, P.; Thacker, J.; Humphrey, T. Pathway utilization in response to a site-specific DNA double-strand break in fission yeast. *EMBO J.* **2003**, *22*, 1419–1430. [CrossRef] [PubMed]
55. Kim, D.U.; Hayles, J.; Kim, D.; Wood, V.; Park, H.O.; Won, M.; Yoo, H.S.; Duhig, T.; Nam, M.; Palmer, G.; et al. Analysis of a genome-wide set of gene deletions in the fission yeast Schizosaccharomyces pombe. *Nat. Biotechnol.* **2010**, *28*, 617–623. [CrossRef] [PubMed]
56. Moss, J.; Tinline-Purvis, H.; Walker, C.A.; Folkes, L.K.; Stratford, M.R.; Hayles, J.; Hoe, K.L.; Kim, D.U.; Park, H.O.; Kearsey, S.E.; et al. Break-induced ATR and Ddb1-Cul4(Cdt)(2) ubiquitin ligase-dependent nucleotide synthesis promotes homologous recombination repair in fission yeast. *Genes Dev.* **2010**, *24*, 2705–2716. [CrossRef]
57. Pai, C.C.; Blaikley, E.; Humphrey, T.C. DNA Double-Strand Break Repair Assay. *Cold Spring Harb. Protoc.* **2018**, *2018*. [CrossRef]
58. Hartsuiker, E.; Vaessen, E.; Carr, A.M.; Kohli, J. Fission yeast Rad50 stimulates sister chromatid recombination and links cohesion with repair. *EMBO J.* **2001**, *20*, 6660–6671. [CrossRef]
59. Jackson, J.A.; Fink, G.R. Gene Conversion between Duplicated Genetic Elements in Yeast. *Nature* **1981**, *292*, 306–311. [CrossRef]
60. Rothstein, R.; Helms, C.; Rosenberg, N. Concerted Deletions and Inversions Are Caused by Mitotic Recombination between Delta-Sequences in Saccharomyces-Cerevisiae. *Mol. Cell. Biol.* **1987**, *7*, 1198–1207. [CrossRef]
61. Macdonald, M.V.; Whitehouse, H.L.K. A Buff Spore Color Mutant in Sordaria-Brevicollis Showing High-Frequency Conversion: 2. Loss of the High-Frequency Conversion. *Genet. Res.* **1983**, *41*, 155–163. [CrossRef]
62. Pukkila, P.J.; Stephens, M.D.; Binninger, D.M.; Errede, B. Frequency and Directionality of Gene Conversion Events Involving the Cyc7-H3 Mutation in Saccharomyces-Cerevisiae. *Genetics* **1986**, *114*, 347–361. [PubMed]

63. Gutz, H. Site Specific Induction of Gene Conversion in schizosaccharomyces pombe. *Genetics* **1971**, *69*, 317–337. [PubMed]
64. Schuchert, P.; Kohli, J. The Ade6-M26 Mutation of Schizosaccharomyces-Pombe Increases the Frequency of Crossing Over. *Genetics* **1988**, *119*, 507–515. [PubMed]
65. Fortunato, E.A.; Osman, F.; Subramani, S. Analysis of spontaneous and double-strand break-induced recombination in rad mutants of S. pombe. *Mutat. Res.* **1996**, *364*, 14–60. [CrossRef]
66. Osman, F.; Fortunato, E.A.; Subramani, S. Double-strand break-induced mitotic intrachromosomal recombination in the fission yeast Schizosaccharomyces pombe. *Genetics* **1996**, *142*, 341–357. [PubMed]
67. Ahamad, N.; Verma, S.K.; Ahmed, S. Activation of Checkpoint Kinase Chk1 by Reactive Oxygen Species Resulting from Disruption of wat1/pop3 in Schizosaccharomyces pombe. *Genetics* **2016**, *204*, 1397–1406. [CrossRef]
68. Bellini, A.; Girard, P.M.; Lambert, S.; Tessier, L.; Sage, E.; Francesconi, S. Stress activated protein kinase pathway modulates homologous recombination in fission yeast. *PLoS ONE* **2012**, *7*, e47987. [CrossRef]
69. Nandi, S.; Whitby, M.C. The ATPase activity of Fml1 is essential for its roles in homologous recombination and DNA repair. *Nucleic Acids Res.* **2012**, *40*, 9584–9595. [CrossRef]
70. Osman, F.; Tsaneva, I.R.; Whitby, M.C.; Doe, C.L. UV irradiation causes the loss of viable mitotic recombinants in Schizosaccharomyces pombe cells lacking the G(2)/M DNA damage checkpoint. *Genetics* **2002**, *160*, 891–908.
71. Bass, K.L.; Murray, J.M.; O'Connell, M.J. Brc1-dependent recovery from replication stress. *J. Cell Sci.* **2012**, *125*, 2753–2764. [CrossRef]
72. Osman, F.; Bjoras, M.; Alseth, I.; Morland, I.; McCready, S.; Seeberg, E.; Tsaneva, I. A new Schizosaccharomyces pombe base excision repair mutant, nth1, reveals overlapping pathways for repair of DNA base damage. *Mol. Microbiol.* **2003**, *48*, 465–480. [CrossRef] [PubMed]
73. Sommariva, E.; Pellny, T.K.; Karahan, N.; Kumar, S.; Huberman, J.A.; Dalgaard, J.Z. Schizosaccharomyces pombe Swi1, Swi3, and Hsk1 are components of a novel S-phase response pathway to alkylation damage. *Mol. Cell. Biol.* **2005**, *25*, 2770–2784. [CrossRef] [PubMed]
74. Yokoyama, M.; Inoue, H.; Ishii, C.; Murakami, Y. The novel gene mus7(+) is involved in the repair of replication-associated DNA damage in fission yeast. *DNA Repair* **2007**, *6*, 770–780. [CrossRef] [PubMed]
75. Ono, Y.; Tomita, K.; Matsuura, A.; Nakagawa, T.; Masukata, H.; Uritani, M.; Ushimaru, T.; Ueno, M. A novel allele of fission yeast rad11 that causes defects in DNA repair and telomere length regulation. *Nucleic Acids Res.* **2003**, *31*, 7141–7149. [CrossRef] [PubMed]
76. Steinacher, R.; Osman, F.; Lorenz, A.; Bryer, C.; Whitby, M.C. Slx8 Removes Pli1-Dependent Protein-SUMO Conjugates Including SUMOylated Topoisomerase I to Promote Genome Stability. *PLoS ONE* **2013**, *8*. [CrossRef] [PubMed]
77. Tsang, E.; Miyabe, I.; Iraqui, I.; Zheng, J.; Lambert, S.A.; Carr, A.M. The extent of error-prone replication restart by homologous recombination is controlled by Exo1 and checkpoint proteins. *J. Cell Sci.* **2014**, *127*, 2983–2994. [CrossRef]
78. Octobre, G.; Lorenz, A.; Loidl, J.; Kohli, J. The Rad52 homologs Rad22 and Rti1 of Schizosaccharomyces pombe are not essential for meiotic interhomolog recombination, but are required for meiotic intrachromosomal recombination and mating-type-related DNA repair. *Genetics* **2008**, *178*, 2399–2412. [CrossRef]
79. Doe, C.L.; Dixon, J.; Osman, F.; Whitby, M.C. Partial suppression of the fission yeast rqh1(-) phenotype by expression of a bacterial Holliday junction resolvase. *EMBO J.* **2000**, *19*, 2751–2762. [CrossRef]
80. Doe, C.L.; Osman, F.; Dixon, J.; Whitby, M.C. The Holliday junction resolvase SpCCE1 prevents mitochondrial DNA aggregation in Schizosaccharomyces pombe. *Mol. Gen. Genet.* **2000**, *263*, 889–897. [CrossRef]
81. Doe, C.L.; Whitby, M.C. The involvement of Srs2 in post-replication repair and homologous recombination in fission yeast. *Nucleic Acids Res.* **2004**, *32*, 1480–1491. [CrossRef]
82. Doe, C.L.; Osman, F.; Dixon, J.; Whitby, M.C. DNA repair by a Rad22-Mus81-dependent pathway that is independent of Rhp51. *Nucleic Acids Res.* **2004**, *32*, 5570–5581. [CrossRef] [PubMed]
83. Osman, F.; Ahn, J.S.; Lorenz, A.; Whitby, M.C. The RecQ DNA helicase Rqh1 constrains Exonuclease 1-dependent recombination at stalled replication forks. *Sci. Rep.* **2016**, *6*, 22837. [CrossRef] [PubMed]
84. Kuzminov, A. Single-strand interruptions in replicating chromosomes cause double-strand breaks. *Proc. Natl. Acad. Sci. USA* **2001**, *98*, 8241–8246. [CrossRef]

85. Asano, S.; Higashitani, A.; Horiuchi, K. Filamentous phage replication initiator protein gpII forms a covalent complex with the 5′ end of the nick it introduced. *Nucleic Acids Res.* **1999**, *27*, 1882–1889. [CrossRef] [PubMed]
86. Dalgaard, J.Z.; Klar, A.J. A DNA replication-arrest site RTS1 regulates imprinting by determining the direction of replication at mat1 in S. pombe. *Genes Dev.* **2001**, *15*, 2060–2068. [CrossRef] [PubMed]
87. Ahn, J.S.; Osman, F.; Whitby, M.C. Replication fork blockage by RTS1 at an ectopic site promotes recombination in fission yeast. *EMBO J.* **2005**, *24*, 2011–2023. [CrossRef]
88. Lorenz, A.; Osman, F.; Folkyte, V.; Sofueva, S.; Whitby, M.C. Fbh1 limits Rad51-dependent recombination at blocked replication forks. *Mol. Cell. Biol.* **2009**, *29*, 4742–4756. [CrossRef]
89. Nguyen, M.O.; Jalan, M.; Morrow, C.A.; Osman, F.; Whitby, M.C. Recombination occurs within minutes of replication blockage by RTS1 producing restarted forks that are prone to collapse. *Elife* **2015**, *4*, e04539. [CrossRef]
90. Sun, W.; Nandi, S.; Osman, F.; Ahn, J.S.; Jakovleska, J.; Lorenz, A.; Whitby, M.C. The FANCM Ortholog Fml1 Promotes Recombination at Stalled Replication Forks and Limits Crossing Over during DNA Double-Strand Break Repair. *Mol. Cell.* **2008**, *32*, 118–128. [CrossRef]
91. Steinacher, R.; Osman, F.; Dalgaard, J.Z.; Lorenz, A.; Whitby, M.C. The DNA helicase Pfh1 promotes fork merging at replication termination sites to ensure genome stability. *Gene Dev.* **2012**, *26*, 594–602. [CrossRef]
92. Osman, F.; Whitby, M.C. Monitoring homologous recombination following replication fork perturbation in the fission yeast Schizosaccharomyces pombe. *Methods Mol. Biol.* **2009**, *521*, 535–552. [CrossRef] [PubMed]
93. Jalan, M.; Oehler, J.; Morrow, C.A.; Osman, F.; Whitby, M.C. Factors affecting template switch recombination associated with restarted DNA replication. *Elife* **2019**, *8*. [CrossRef] [PubMed]
94. McFarlane, R.J.; Whitehall, S.K. tRNA genes in eukaryotic genome organization and reorganization. *Cell Cycle* **2009**, *8*, 3102–3106. [CrossRef] [PubMed]
95. Sofueva, S.; Osman, F.; Lorenz, A.; Steinacher, R.; Castagnetti, S.; Ledesma, J.; Whitby, M.C. Ultrafine anaphase bridges, broken DNA and illegitimate recombination induced by a replication fork barrier. *Nucleic Acids Res.* **2011**, *39*, 6568–6584. [CrossRef] [PubMed]
96. Tamang, S.; Kishkevich, A.; Morrow, C.A.; Osman, F.; Jalan, M.; Whitby, M.C. The PCNA unloader Elg1 promotes recombination at collapsed replication forks in fission yeast. *Elife* **2019**, *8*, e47277. [CrossRef]
97. Watson, A.T.; Werler, P.; Carr, A.M. Regulation of gene expression at the fission yeast Schizosaccharomyces pombe urg1 locus. *Gene* **2011**, *484*, 76–86. [CrossRef]
98. Forsburg, S.L. Comparison of Schizosaccharomyces-Pombe Expression Systems. *Nucleic Acids Res.* **1993**, *21*, 2955–2956. [CrossRef]
99. Maundrell, K. Thiamine-repressible expression vectors pREP and pRIP for fission yeast. *Gene* **1993**, *123*, 127–130. [CrossRef]
100. Muller, S.; Sandal, T.; Kamp-Hansen, P.; Dalboge, H. Comparison of expression systems in the yeasts Saccharomyces cerevisiae, Hansenula polymorpha, Klyveromyces lactis, Schizosaccharomyces pombe and Yarrowia lipolytica. Cloning of two novel promoters from Yarrowia lipolytica. *Yeast* **1998**, *14*, 1267–1283. [CrossRef]
101. Watson, A.T.; Daigaku, Y.; Mohebi, S.; Etheridge, T.J.; Chahwan, C.; Murray, J.M.; Carr, A.M. Optimisation of the Schizosaccharomyces pombe urg1 Expression System. *PLoS ONE* **2013**, *8*, e83800. [CrossRef]
102. Sunder, S.; Greeson-Lott, N.T.; Runge, K.W.; Sanders, S.L. A new method to efficiently induce a site-specific double-strand break in the fission yeast Schizosaccharomyces pombe. *Yeast* **2012**, *29*, 275–291. [CrossRef] [PubMed]
103. Zilio, N.; Wehrkamp-Richter, S.; Boddy, M.N. A new versatile system for rapid control of gene expression in the fission yeast Schizosaccharomyces pombe. *Yeast* **2012**, *29*, 425–434. [CrossRef]
104. Lucas, B.E.; McPherson, M.T.; Hawk, T.M.; Wilson, L.N.; Kroh, J.M.; Hickman, K.G.; Fitzgerald, S.R.; Disbennett, W.M.; Rollins, P.D.; Hylton, H.M.; et al. An Assay to Study Intra-Chromosomal Deletions in Yeast. *Methods Protoc.* **2019**, *2*. [CrossRef] [PubMed]
105. Lambert, S.; Watson, A.; Sheedy, D.M.; Martin, B.; Carr, A.M. Gross chromosomal rearrangements and elevated recombination at an inducible site-specific replication fork barrier. *Cell* **2005**, *121*, 689–702. [CrossRef] [PubMed]
106. Saada, A.A.; Teixeira-Silva, A.; Iraqui, I.; Costes, A.; Hardy, J.; Paoletti, G.; Freon, K.; Lambert, S.A.E. Unprotected Replication Forks Are Converted into Mitotic Sister Chromatid Bridges. *Mol. Cell* **2017**, *66*, 398. [CrossRef] [PubMed]

107. Mizuno, K.; Lambert, S.; Baldacci, G.; Murray, J.M.; Carr, A.M. Nearby inverted repeats fuse to generate acentric and dicentric palindromic chromosomes by a replication template exchange mechanism. *Gene Dev.* **2009**, *23*, 2876–2886. [CrossRef]
108. Mizuno, K.; Miyabe, I.; Schalbetter, S.A.; Carr, A.M.; Murray, J.M. Recombination-restarted replication makes inverted chromosome fusions at inverted repeats. *Nature* **2013**, *493*, 246–249. [CrossRef]
109. Mohebi, S.; Mizuno, K.; Watson, A.; Carr, A.M.; Murray, J.M. Checkpoints are blind to replication restart and recombination intermediates that result in gross chromosomal rearrangements. *Nat. Commun.* **2015**, *6*, 6357. [CrossRef]
110. Iraqui, I.; Chekkal, Y.; Jmari, N.; Pietrobon, V.; Freon, K.; Costes, A.; Lambert, S.A.E. Recovery of Arrested Replication Forks by Homologous Recombination Is Error-Prone. *Plos Genetics* **2012**, *8*, e1002976. [CrossRef]
111. Lambert, S.; Mizuno, K.; Blaisonneau, J.; Martineau, S.; Chanet, R.; Freon, K.; Murray, J.M.; Carr, A.M.; Baldacci, G. Homologous Recombination Restarts Blocked Replication Forks at the Expense of Genome Rearrangements by Template Exchange. *Mol. Cell* **2010**, *39*, 346–359. [CrossRef]
112. Teixeira-Silva, A.; Ait Saada, A.; Hardy, J.; Iraqui, I.; Nocente, M.C.; Freon, K.; Lambert, S.A.E. The end-joining factor Ku acts in the end-resection of double strand break-free arrested replication forks. *Nat. Commun.* **2017**, *8*, 1982. [CrossRef] [PubMed]
113. Arcangioli, B.; Roseaulin, L.; Holmes, A. Mating-Type Switching in S. Pombe. In *Molecular Genetics of Recombination*; Springer: Berlin, Germany, 2007; pp. 95–133.
114. Leupold, U. Studies on recombination in Schizosaccharomyces pombe. *Cold Spring Harb. Symp. Quant. Biol.* **1958**, *23*, 161–170. [CrossRef]
115. Egel, R. Genes involved in mating type expression of fission yeast. *Mol. Gen. Genet.* **1973**, *122*, 339–343. [CrossRef] [PubMed]
116. Egel, R.; Gutz, H. Gene activation by copy transposition in mating-type switching of a homothallic fission yeast. *Curr. Genet.* **1981**, *3*, 5–12. [CrossRef] [PubMed]
117. Egel, R.; Beach, D.H.; Klar, A.J. Genes required for initiation and resolution steps of mating-type switching in fission yeast. *Proc. Natl Acad. Sci. USA* **1984**, *81*, 3481–3485. [CrossRef]
118. Egel, R. Two tightly linked silent cassettes in the mating-type region of Schizosaccharomyces pombe. *Curr. Genet.* **1984**, *8*, 199–203. [CrossRef]
119. Beach, D.H.; Klar, A.J. Rearrangements of the transposable mating-type cassettes of fission yeast. *EMBO J.* **1984**, *3*, 603–610. [CrossRef]
120. Klar, A.J. Lessons learned from studies of fission yeast mating-type switching and silencing. *Annu. Rev. Genet.* **2007**, *41*, 213–236. [CrossRef]
121. Thon, G.; Maki, T.; Haber, J.E.; Iwasaki, H. Mating-type switching by homology-directed recombinational repair: A matter of choice. *Curr. Genet.* **2019**, *65*, 351–362. [CrossRef]
122. Hanson, S.J.; Wolfe, K.H. An Evolutionary Perspective on Yeast Mating-Type Switching. *Genetics* **2017**, *206*, 9–32. [CrossRef]
123. Gutz, H.; Doe, F.J. Two Different h Mating Types in schizosaccharomyces pombe. *Genetics* **1973**, *74*, 563–569. [PubMed]
124. Egel, R. Frequency of mating-type switching in homothallic fission yeast. *Nature* **1977**, *266*, 172–174. [CrossRef]
125. Lee, C.S.; Haber, J.E. Mating-type Gene Switching in Saccharomyces cerevisiae. *Microbiol. Spectr.* **2015**, *3*. [CrossRef]
126. Vengrova, S.; Dalgaard, J.Z. RNase-sensitive DNA modification(s) initiates S. pombe mating-type switching. *Gene Dev.* **2004**, *18*, 794–804. [CrossRef]
127. Vengrova, S.; Dalgaard, J.Z. The wild-type Schizosaccharomyces pombe mat1 imprint consists of two ribonucleotides. *EMBO Rep.* **2006**, *7*, 59–65. [CrossRef] [PubMed]
128. Singh, B.; Bisht, K.K.; Upadhyay, U.; Kushwaha, A.C.; Nanda, J.S.; Srivastava, S.; Saini, J.K.; Klar, A.J.S.; Singh, J. Role of Cdc23/Mcm10 in generating the ribonucleotide imprint at the mat1 locus in fission yeast. *Nucleic Acids Res.* **2019**, *47*, 3422–3433. [CrossRef] [PubMed]
129. Kaykov, A.; Holmes, A.M.; Arcangioli, B. Formation, maintenance and consequences of the imprint at the mating-type locus in fission yeast. *EMBO J.* **2004**, *23*, 930–938. [CrossRef] [PubMed]
130. Dalgaard, L.Z.; Klar, A.J.S. Orientation of DNA replication establishes mating-type switching pattern in S-pombe. *Nature* **1999**, *400*, 181–184. [CrossRef]

131. Arcangioli, B. A site- and strand-specific DNA break confers asymmetric switching potential in fission yeast. *EMBO J.* **1998**, *17*, 4503–4510. [CrossRef]
132. Arcangioli, B.; de Lahondes, R. Fission yeast switches mating type by a replication-recombination coupled process. *Embo J.* **2000**, *19*, 1389–1396. [CrossRef]
133. Holmes, A.M.; Kaykov, A.; Arcangioli, B. Molecular and cellular dissection of mating-type switching steps in Schizosaccharomyces pombe. *Mol. Cell. Biol.* **2005**, *25*, 303–311. [CrossRef] [PubMed]
134. Vengrova, S.; Codlin, S.; Dalgaard, J.Z. RTS1—an eukaryotic terminator of replication. *Int. J. Biochem. Cell. B* **2002**, *34*, 1031–1034. [CrossRef]
135. Klar, A.J.S.; Ishikawa, K.; Moore, S. A Unique DNA Recombination Mechanism of the Mating/Cell-type Switching of Fission Yeasts: A Review. *Microbiol. Spectr.* **2014**, *2*, 5. [CrossRef]
136. Roseaulin, L.; Yamada, Y.; Tsutsui, Y.; Russell, P.; Iwasaki, H.; Arcangioli, B. Mus81 is essential for sister chromatid recombination at broken replication forks. *EMBO J.* **2008**, *27*, 1378–1387. [CrossRef]
137. Styrkarsdottir, U.; Egel, R.; Nielsen, O. The smt-0 mutation which abolishes mating-type switching in fission yeast is a deletion. *Curr. Genet.* **1993**, *23*, 184–186. [CrossRef]
138. Klar, A.J.; Miglio, L.M. Initiation of meiotic recombination by double-strand DNA breaks in S. pombe. *Cell* **1986**, *46*, 725–731. [CrossRef]
139. Zhu, M.; Zhao, H.; Limbo, O.; Russell, P. Mre11 complex links sister chromatids to promote repair of a collapsed replication fork. *Proc. Natl. Acad. Sci. USA* **2018**, *115*, 8793–8798. [CrossRef]
140. Zhao, H.; Zhu, M.; Limbo, O.; Russell, P. RNase H eliminates R-loops that disrupt DNA replication but is nonessential for efficient DSB repair. *EMBO Rep.* **2018**, *19*. [CrossRef]
141. Gutz, H.; Schmidt, H. Switching genes in Schizosaccharomyces pombe. *Curr. Genet.* **1985**, *9*, 325–331. [CrossRef]
142. Inagawa, T.; Yamada-Inagawa, T.; Eydmann, T.; Mian, I.S.; Wang, T.S.; Dalgaard, J.Z. Schizosaccharomyces pombe Rtf2 mediates site-specific replication termination by inhibiting replication restart. *Proc. Natl. Acad. Sci. USA* **2009**, *106*, 7927–7932. [CrossRef]
143. Allshire, R.C.; Ekwall, K. Epigenetic Regulation of Chromatin States in Schizosaccharomyces pombe. *Cold Spring Harb. Perspect. Biol.* **2015**, *7*, a018770. [CrossRef] [PubMed]
144. Volpe, T.A.; Kidner, C.; Hall, I.M.; Teng, G.; Grewal, S.I.; Martienssen, R.A. Regulation of heterochromatic silencing and histone H3 lysine-9 methylation by RNAi. *Science* **2002**, *297*, 1833–1837. [CrossRef] [PubMed]
145. Jia, S.; Noma, K.; Grewal, S.I. RNAi-independent heterochromatin nucleation by the stress-activated ATF/CREB family proteins. *Science* **2004**, *304*, 1971–1976. [CrossRef] [PubMed]
146. Verdel, A.; Jia, S.; Gerber, S.; Sugiyama, T.; Gygi, S.; Grewal, S.I.; Moazed, D. RNAi-mediated targeting of heterochromatin by the RITS complex. *Science* **2004**, *303*, 672–676. [CrossRef]
147. Thon, G.; Klar, A.J. The clr1 locus regulates the expression of the cryptic mating-type loci of fission yeast. *Genetics* **1992**, *131*, 287–296.
148. Ekwall, K.; Ruusala, T. Mutations in rik1, clr2, clr3 and clr4 genes asymmetrically derepress the silent mating-type loci in fission yeast. *Genetics* **1994**, *136*, 53–64.
149. Thon, G.; Cohen, A.; Klar, A.J. Three additional linkage groups that repress transcription and meiotic recombination in the mating-type region of Schizosaccharomyces pombe. *Genetics* **1994**, *138*, 29–38.
150. Nabeshima, K.; Nakagawa, T.; Straight, A.F.; Murray, A.; Chikashige, Y.; Yamashita, Y.M.; Hiraoka, Y.; Yanagida, M. Dynamics of centromeres during metaphase-anaphase transition in fission yeast: Dis1 is implicated in force balance in metaphase bipolar spindle. *Mol. Biol. Cell* **1998**, *9*, 3211–3225. [CrossRef]
151. Du, L.L.; Nakamura, T.M.; Moser, B.A.; Russell, P. Retention but not recruitment of Crb2 at double-strand breaks requires Rad1 and Rad3 complexes. *Mol. Cell. Biol.* **2003**, *23*, 6150–6158. [CrossRef]
152. Du, L.L.; Nakamura, T.M.; Russell, P. Histone modification-dependent and -independent pathways for recruitment of checkpoint protein Crb2 to double-strand breaks. *Genes Dev.* **2006**, *20*, 1583–1596. [CrossRef]
153. Sofueva, S.; Du, L.L.; Limbo, O.; Williams, J.S.; Russell, P. BRCT domain interactions with phospho-histone H2A target Crb2 to chromatin at double-strand breaks and maintain the DNA damage checkpoint. *Mol. Cell. Biol.* **2010**, *30*, 4732–4743. [CrossRef] [PubMed]
154. Nakamura, T.M.; Moser, B.A.; Du, L.L.; Russell, P. Cooperative control of Crb2 by ATM family and Cdc2 kinases is essential for the DNA damage checkpoint in fission yeast. *Mol. Cell. Biol.* **2005**, *25*, 10721–10730. [CrossRef] [PubMed]

155. Limbo, O.; Chahwan, C.; Yamada, Y.; de Bruin, R.A.M.; Wittenberg, C.; Russell, P. Ctp1 is a cell-cycle-regulated protein that functions with Mre11 complex to control double-strand break repair by homologous recombination. *Mol. Cell* **2007**, *28*, 134–146. [CrossRef] [PubMed]
156. Williams, R.S.; Moncalian, G.; Williams, J.S.; Yamada, Y.; Limbo, O.; Shin, D.S.; Groocock, L.M.; Cahill, D.; Hitomi, C.; Guenther, G.; et al. Mre11 dimers coordinate DNA end bridging and nuclease processing in double-strand-break repair. *Cell* **2008**, *135*, 97–109. [CrossRef] [PubMed]
157. Limbo, O.; Porter-Goff, M.E.; Rhind, N.; Russell, P. Mre11 Nuclease Activity and Ctp1 Regulate Chk1 Activation by Rad3(ATR) and Tel1(ATM) Checkpoint Kinases at Double-Strand Breaks. *Mol. Cell. Biol.* **2011**, *31*, 573–583. [CrossRef] [PubMed]
158. Limbo, O.; Moiani, D.; Kertokalio, A.; Wyman, C.; Tainer, J.A.; Russell, P. Mre11 ATLD17/18 mutation retains Tel1/ATM activity but blocks DNA double-strand break repair. *Nucleic Acids Res.* **2012**, *40*, 11435–11449. [CrossRef] [PubMed]
159. Wei, Y.; Wang, H.T.; Zhai, Y.; Russell, P.; Du, L.L. Mdb1, a Fission Yeast Homolog of Human MDC1, Modulates DNA Damage Response and Mitotic Spindle Function. *PLoS ONE* **2014**, *9*, e97028. [CrossRef]
160. Limbo, O.; Yamada, Y.; Russell, P. Mre11-Rad50-dependent activity of ATM/Tel1 at DNA breaks and telomeres in the absence of Nbs1. *Mol. Biol. Cell* **2018**, *29*, 1389–1399. [CrossRef]
161. Langerak, P.; Mejia-Ramirez, E.; Limbo, O.; Russell, P. Release of Ku and MRN from DNA Ends by Mre11 Nuclease Activity and Ctp1 Is Required for Homologous Recombination Repair of Double-Strand Breaks. *PLoS Genet.* **2011**, *7*, e1002271. [CrossRef]
162. Zierhut, C.; Diffley, J.F.X. Break dosage, cell cycle stage and DNA replication influence DNA double strand break response. *EMBO J.* **2008**, *27*, 1875–1885. [CrossRef]
163. Leland, B.A.; King, M.C. Using LacO Arrays to Monitor DNA Double-Strand Break Dynamics in Live Schizosaccharomyces pombe Cells. In *Cancer Genomics and Proteomics: Methods and Protocols*, 2nd ed.; Humana Press: New York, NY, USA, 2014; Volume 1176, pp. 127–141.
164. Yu, Y.; Ren, J.Y.; Zhang, J.M.; Suo, F.; Fang, X.F.; Wu, F.; Du, L.L. A proteome-wide visual screen identifies fission yeast proteins localizing to DNA double-strand breaks. *DNA Repair* **2013**, *12*, 433–443. [CrossRef] [PubMed]
165. Matsuyama, A.; Arai, R.; Yashiroda, Y.; Shirai, A.; Kamata, A.; Sekido, S.; Kobayashi, Y.; Hashimoto, A.; Hamamoto, M.; Hiraoka, Y.; et al. ORFeome cloning and global analysis of protein localization in the fission yeast Schizosaccharomyces pombe. *Nat. Biotechnol.* **2006**, *24*, 841–847. [CrossRef]
166. Goedecke, W.; Pfeiffer, P.; Vielmetter, W. Nonhomologous DNA end joining in Schizosaccharomyces pombe efficiently eliminates DNA double-strand-breaks from haploid sequences. *Nucleic Acids Res.* **1994**, *22*, 2094–2101. [CrossRef] [PubMed]
167. Manolis, K.G.; Nimmo, E.R.; Hartsuiker, E.; Carr, A.M.; Jeggo, P.A.; Allshire, R.C. Novel functional requirements for non-homologous DNA end joining in Schizosaccharomyces pombe. *EMBO J.* **2001**, *20*, 210–221. [CrossRef] [PubMed]
168. Boulton, S.J.; Jackson, S.P. Saccharomyces cerevisiae Ku70 potentiates illegitimate DNA double-strand break repair and serves as a barrier to error-prone DNA repair pathways. *EMBO J.* **1996**, *15*, 5093–5103. [CrossRef] [PubMed]
169. Hentges, P.; Ahnesorg, P.; Pitcher, R.S.; Bruce, C.K.; Kysela, B.; Green, A.J.; Bianchi, J.; Wilson, T.E.; Jackson, S.P.; Doherty, A.J. Evolutionary and functional conservation of the DNA non-homologous end-joining protein, XLF/cernunnos. *J. Biol. Chem.* **2006**, *281*, 37517–37526. [CrossRef]
170. Decottignies, A. Capture of extranuclear DNA at fission yeast double-strand breaks. *Genetics* **2005**, *171*, 1535–1548. [CrossRef]
171. Li, J.; Yu, Y.; Suo, F.; Sun, L.L.; Zhao, D.; Du, L.L. Genome-wide Screens for Sensitivity to Ionizing Radiation Identify the Fission Yeast Nonhomologous End Joining Factor Xrc4. *G3-Genes Genom Genet.* **2014**, *4*, 1297–1306. [CrossRef]
172. Li, P.; Li, J.; Li, M.; Dou, K.; Zhang, M.J.; Suo, F.; Du, L.L. Multiple end joining mechanisms repair a chromosomal DNA break in fission yeast. *DNA Repair* **2012**, *11*, 120–130. [CrossRef]
173. Li, Y.; Wang, J.; Zhou, G.; Lajeunesse, M.; Le, N.; Stawicki, B.N.; Corcino, Y.L.; Berkner, K.L.; Runge, K.W. Nonhomologous End-Joining with Minimal Sequence Loss Is Promoted by the Mre11-Rad50-Nbs1-Ctp1 Complex in Schizosaccharomyces pombe. *Genetics* **2017**, *206*, 481–496. [CrossRef]

174. Almeida, H.; Godinho Ferreira, M. Spontaneous telomere to telomere fusions occur in unperturbed fission yeast cells. *Nucleic Acids Res.* **2013**, *41*, 3056–3067. [CrossRef] [PubMed]
175. Van, H.T.; Santos, M.A. Histone modifications and the DNA double-strand break response. *Cell Cycle* **2018**, *17*, 2399–2410. [CrossRef] [PubMed]
176. Bader, A.S.; Hawley, B.R.; Wilczynska, A.; Bushell, M. The roles of RNA in DNA double-strand break repair. *Br. J. Cancer* **2020**. [CrossRef] [PubMed]